

**Electrical Resistivity Imaging
Barite Hill Gold Mine
McCormick County
South Carolina
Prepared for:
Black & Veatch Special Projects Corporation

September 22, 2011**

**Electrical Resistivity Imaging
Barite Hill Gold Mine
McCormick County, South Carolina**

TABLE OF CONTENTS

<u>Section</u>	<u>Page</u>
Signature Page	ii
Executive Summary	iii
1.0 Introduction.....	1
1.1 Background.....	1
2.0 Equipment and Methodology.....	1
2.1 Supersting/Swift R8 Resistivity Meter	2
3.0 Field Procedures.....	3
4.0 Data Interpretation and Results.....	4

Figures

Figure 1 ERI Profile Locations
Figure 2 Interpreted Lateral and Vertical Extent of the Rainsford Pit
Figure 3 ERI Interpretations for Profile 5

Appendices

Appendix 1 Inverted ERI Profiles
Appendix 2 Raw Data, Calculated Data and ERI Models

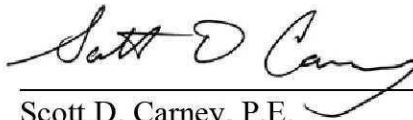
Signature Page

This report, entitled "Electrical Resistivity Imaging, Barite Hill Gold Mine, McCormick County, South Carolina" has been prepared for Black & Veatch Special Project Corporation located in Arvada, Colorado. It has been prepared under the supervision of Mr. Jorgen Bergstrom at the request of and for the exclusive use of Black & Veatch Special Project Corporation. This report has been prepared in accordance with accepted quality control practices and has been reviewed by the undersigned.

GEL Geophysics, LLC
A Member of the GEL Group, Inc.



Jorgen Bergstrom
Senior Geophysicist



Scott D. Carney, P.E.
Director

September 22, 2011
Date

Electrical Resistivity Imaging
Barite Hill Gold Mine
McCormick County, South Carolina

EXECUTIVE SUMMARY

GEL Geophysics performed an electrical resistivity imaging (ERI) investigation at the Barite Hill Gold Mine in McCormick County, South Carolina on August 30 to September 2, 2011. This investigation was performed for Black & Veatch Special Project Corporation (BVSPC) to aid in characterizing the subsurface along select profiles at the site. The investigation entailed the collection, processing, presentation, and interpretation of resistivity and induced polarization (IP) data. The objectives of the geophysical investigation were to:

1. Identify the lateral and vertical extent of the backfilled Rainsford Pit.
2. Identify potential preferential ground water pathways in bedrock near the Main Pit.

Rainsford Pit data was interpreted mainly by the use of the resistivity data since the pit did not exhibit a significant IP contrast with the surrounding rock. The pit appears to exhibit a fairly low resistivity from the groundwater table to the bottom of the pit. There is an area downstream from the pit (southeast of the pit) that also exhibits low resistivity, presumably due to leachate from the pit. Due to the similarities in response from the pit material and the leachate, determination of the vertical and horizontal extent of the pit was not well defined in the southeast. Based on resistivity data, the deepest part of the pit was found to be approximately 80 feet.

The Main pit data was also interpreted mainly by the use of resistivity data. Leachate appears to be present in the groundwater from the groundwater table to a depth of approximately 60 feet below the groundwater table. Leachate may reach deeper into the bedrock along major fracture zones, such as the one detected in the ERI data.

The ground surface at all five profile locations was found to be very resistive resulting in low output currents and consequently noisy data. GEL Geophysics attempted to mitigate these difficulties by pouring saltwater over the electrodes prior to commencing data collection. This method reduced the contact resistance by approximately 50 percent at most electrodes (from approximately 10,000 Ohm to approximately 5,000 Ohm for the locations with the highest contact resistance). However, a fairly large percentage of the data points (typically 40-60%) were still too noisy and subsequently removed prior to inversion. Although this had a negative effect on the modeling process, the remaining dataset were, in most cases, sufficient for interpretation.

Although geophysical methods provide a high level for the assurance for the location of subsurface objects, the possibility exists that not all features were identified due to the site conditions and limitations of the ERI method.

Electrical Resistivity Imaging
Barite Hill Gold Mine
McCormick County, South Carolina

1.0 INTRODUCTION

GEL Geophysics performed an electrical resistivity imaging (ERI) investigation at the Barite Hill Gold Mine in McCormick County, South Carolina on August 30 to September 2, 2011. This investigation was performed for Black & Veatch Special Project Corporation (BVSPC) to aid in characterizing the subsurface along select profiles at the site.

1.1 Background

BVSPC is currently involved in environmental site investigations at the former Barite Hill Gold Mine. These investigations involve determining sources and potential migration paths for groundwater contamination at the site. The primary contaminants are various metals due to the presence of acid-generating sulfide minerals. To support this investigation, BVSPC invited GEL Geophysics to conduct a geophysical investigation of the site using ERI techniques. The objectives of the geophysical investigation were to:

1. Identify the lateral and vertical extent of the backfilled Rainsford Pit.
2. Identify potential preferential ground water pathways in bedrock near the Main Pit.

The investigation entailed the collection, processing, presentation, and interpretation of resistivity and induced polarization (IP) data.

2.0 EQUIPMENT AND METHODOLOGY

For this investigation GEL Geophysics used Advanced Geosciences, Inc.'s SuperSting/Swift R8 resistivity meter configured with 56 electrodes. Positioning data (horizontal and elevation) was provided by a Trimble 5800 RTK/GPS system for areas

without tree canopies (Profiles 1-4) and a Trimble Geodimeter 600 total station for areas with tree canopies (Profile 5). The total station data was tied into South Carolina State Plane coordinates and true elevations by using known coordinates for a monitoring well (MW-55) provided by BVSPC, and RTK/GPS points collected in open areas next to Profile 5. The following is a brief introduction to the various geophysical equipment used at the site.

2.1 SuperSting/Swift R8 Resistivity Meter

Electrical resistivity surveying is an active geophysical technique that involves the introduction of a known amount of current into the ground and subsequently measuring the earth's response in order to measure variations in their respective electrical potentials. By introducing a known amount of current into the ground and subsequently measuring the voltage potential, the resistivity of a particular volume of earth is measured. It is important to note that actual ground resistivity is not measured during a resistivity survey but rather the apparent resistivity. Actual resistivities are later determined through the inversion process.

Resistivity methods typically require that a series of small current and potential electrodes be pushed into the ground in various configurations. The electrodes are connected to a transmitter/recording instrument that generates the induced current and stores the measurements for later processing and analysis. The R8 version of the SuperSting Resistivity System measures eight electrode combinations simultaneously, thereby reducing measuring time compared with standard one-channel systems. The configuration of the electrodes is dependent on the objectives of the investigation (i.e., vertical soil and bedrock profiling, contaminant mapping, or fracture mapping). The most commonly employed arrays for resistivity surveying are the Wenner, Schlumberger, and Dipole-Dipole. This ERI investigation was conducted using Dipole-Dipole and Wenner arrays with 7.5 meter electrode separation.

Pseudodepth sections are developed by increasing the spacing between the potential electrode dipole and the current electrode dipole in steps. Since many underground features have electrical properties that differ from their surroundings, electrical imaging can be used to detect and delineate a large array of targets. These include: clay layers,

sand or gravel lenses, the top-of-rock and rock pinnacles or float blocks, saltwater intrusion, leachate plumes, NAPLs, hydrocarbons, dam seepage, mineralized zones, water-bearing fractures, buried foundation elements, waste disposal pits or trenches, graves, mines, tunnels, caves, ice or permafrost thicknesses, and more.

For some targets, recording the IP or chargeability improves detection and discrimination. IP measures the ability of the subsurface to hold a charge like a capacitor by measuring a residual potential after interrupting the current abruptly. Common contributors to IP anomalies are clay minerals (membrane polarization) and metallic minerals (mainly sulfide minerals). The IP effect is called chargeability and is measured in milli-seconds (ms).

The combined results of various electrode spacings are plotted as a pseudodepth section or contour map of apparent resistivity and chargeability versus depth. Inversion of the pseudodepth sections is required to convert the section to actual resistivity and chargeability cross-sections. GEL Geophysics used EarthImager 2D by Advanced Geosciences Inc., which is an industry standard resistivity and IP inversion software.

3.0 FIELD PROCEDURES

All of GEL Geophysics field activities were supervised by a senior geophysicist and observed by BVSPC technical personnel. ERI data were collected along five profiles at the site; four at the former Rainsford Pit and one next to the Main Pit (Figure 1). A total length of 3,027 feet of ERI profiles was collected. An electrode spacing of 7.5 meter (24.6 feet) was used for all profiles. The ground surface at all five profile locations was found to be very resistive resulting in low output currents and noisy data. GEL Geophysics attempted to mitigate these difficulties by pouring saltwater over the electrodes prior to commencing data collection. This method reduced the contact resistance by approximately 50 percent at most electrodes (from approximately 10,000 Ohm to approximately 5,000 Ohm for the locations with the highest contact resistance). However, a large percentage of the data points (typically 40-60%) were still too noisy and subsequently removed prior to inversion. The remaining data was still, in most cases, sufficient for interpretation. The remaining data points (black dots) are plotted in pseudosections on Appendix 2 (top graph). A lower density of data point will lead to

lower resolution and some equivalence issues (e.g. a smaller body with resistivity much higher than the background will give the same response as a larger body with resistivity only slightly higher than the background).

Both Wenner and Dipole-Dipole arrays were used on all profiles since the data provided with the two arrays were found to complement each other well and to mitigate the difficult site conditions mentioned above. Both standard resistivity data and IP data was collected on all profiles. At the completion of the ERI investigation, GEL Geophysics located the horizontal and vertical position of start and end point of each resistivity profile as well as a majority of the electrodes. The electrode positioning data was used in order to incorporate surface elevation variations into the data processing. The data were converted to South Carolina State Plane, US Survey foot coordinate system. The profile locations in South Carolina State Plane system are shown on Figure 1.

4.0 DATA INTERPRETATION AND RESULTS

Following the completion of the data collection, the ERI data were inverted to resistivity and chargeability cross sections using EarthImager 2D. Noisy data points and data points with negative resistivity values were deleted from the data set prior to the inversion process. The collected data was compared with calculated data using the final inverted profile to ensure good correlation (Appendix 2). Data from all profiles were interpreted mainly by the use of the resistivity data.

The inverted profiles with interpretations are shown in Appendix 1. For profiles 1-4, which were collected at the Rainsford Pit, crossing profiles as well as the interpreted edge of the Rainsford Pit are shown on the profiles. The bottom of the Rainsford Pit was most clearly defined in profile 4 (located along the long axes of the pit). GEL Geophysics therefore used the interpreted bottom of the pit from profile 4 as the starting point for determining the bottom of the pit in the crossing profiles. Below the ground water table, the Rainsford Pit exhibited low resistivity (less than 50 Ohm-m), while most of the surrounding rock exhibited higher resistivity (more than 200 Ohm-m). Some of the rock down-gradient from the pit (southeast) also exhibits very low resistivity (less than 50 Ohm-m), potentially due to leachate from the pit. Above the ground water table

the Rainsford Pit exhibited low to high resistivity (less than 50 Ohm-m to more than 500 Ohm-m), similar to the surrounding rock. GEL Geophysics therefore extrapolated the edge detected below the groundwater surface to the ground surface. The IP response from the pit material varied from low to high, similar to the surrounding rock. IP was therefore not very useful for identifying the edges of the pit. Due to the similarities in response from the pit material and the leachate, determination of the vertical and horizontal extent of the pit was not well defined in the southeast. GEL Geophysics suggests that some borings be conducted in the area to verify the geophysical interpretation of the data. The interpreted location of the pit and depth to the bottom of the pit from the profiles were combined into a contour map shown on Figure 2. Based on resistivity data, the deepest part of the pit was found to be approximately 80 feet.

Profile 5 was collected west of the Main pit as shown on Figure 3. Interpretation of the resistivity data is shown superimposed on the inverted profile in Appendix 1 and on Figure 3. BVSPC found leachate on the ground surface in one of low spots along Profile 5. The location of the surface leachate is shown Figure 3. Based on the resistivity data, leachate from the Main Pit seems to be mostly concentrated to the upper 60 feet below the ground water table. Leachate may reach deeper into the bedrock along major fracture zones, such as the one shown on Profile 5 and Figure 3.

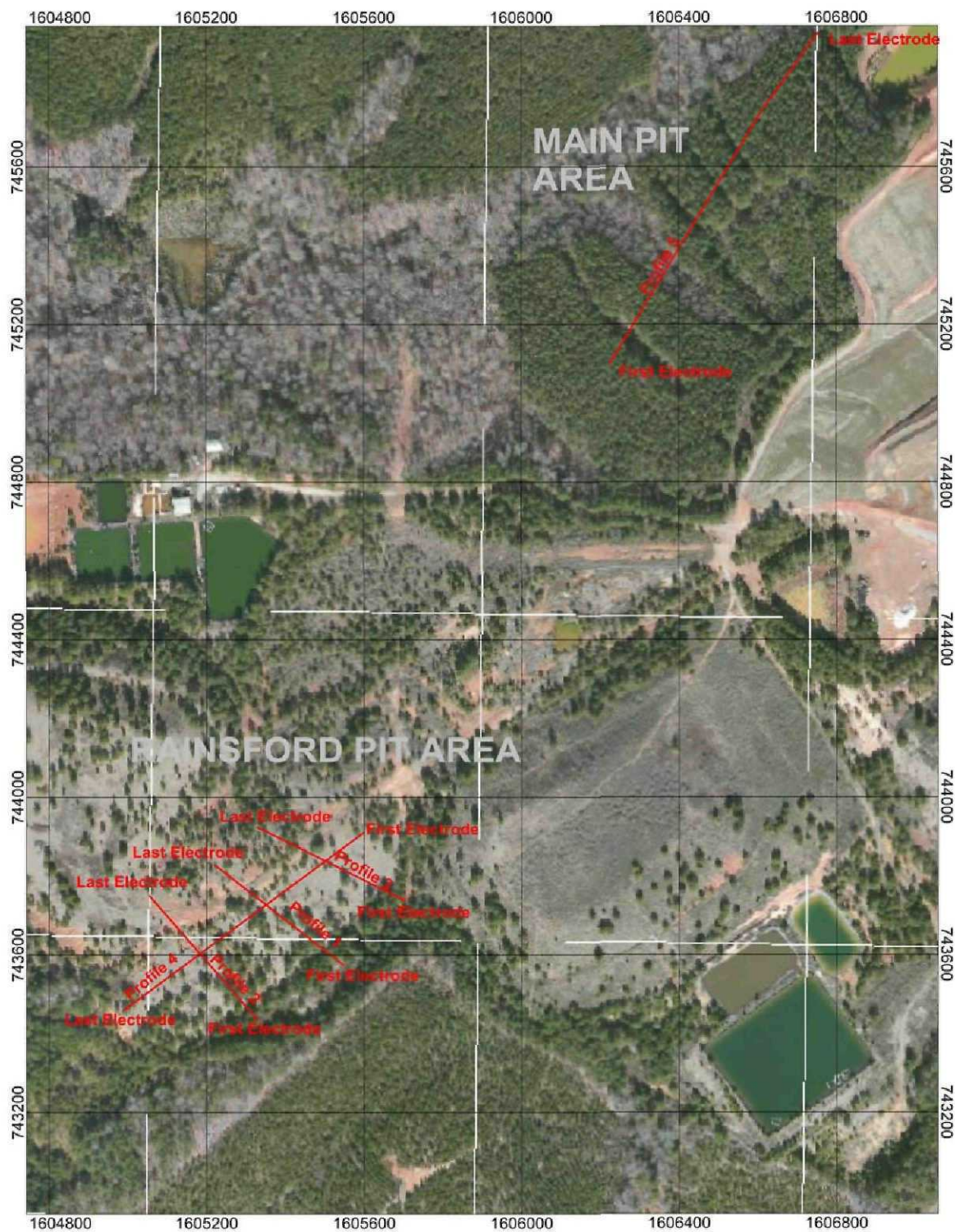
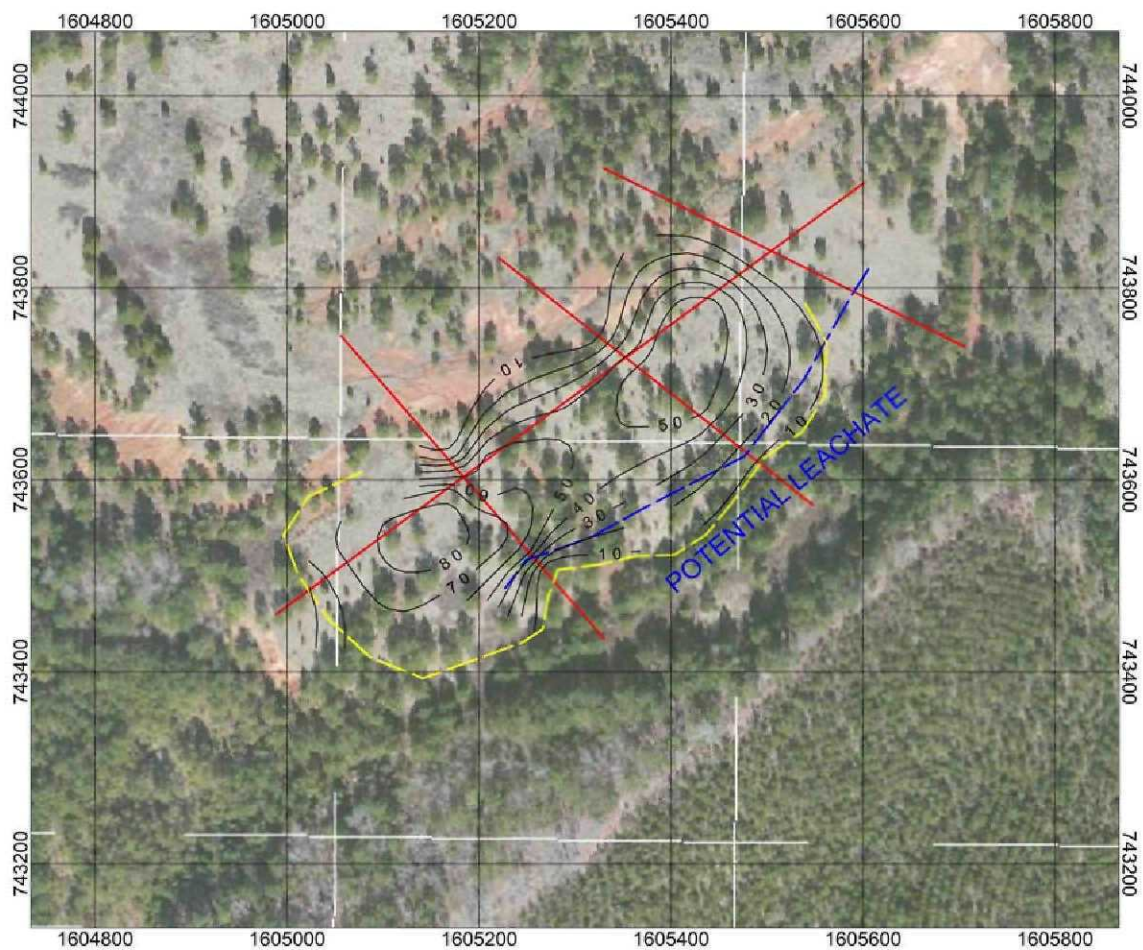


FIGURE 1 ERI PROFILE LOCATIONS

250 0 250 500
 US survey foot Scale: 1"=400'
 WGS 84 / South Carolina CS83



LEGEND

- ERI PROFILE LOCATION
- 10 — INTERPRETED DEPTH TO THE BOTTOM OF THE RAINSFORD PIT (FEET)
- - - HORIZONTAL EXTENT OF THE RAINSFORD PIT NOT WELL DEFINED ALONG LINE
- - - POTENTIAL LEACHATE DETECTED FROM LINE TO SOUTH EAST END OF PROFILES

FIGURE 2 INTERPRETED LATERAL AND VERTICAL EXTENT OF THE RAINSFORD PIT

100 0 100 200
 US survey foot Scale: 1"=200'
 WGS 84 / South Carolina CS83



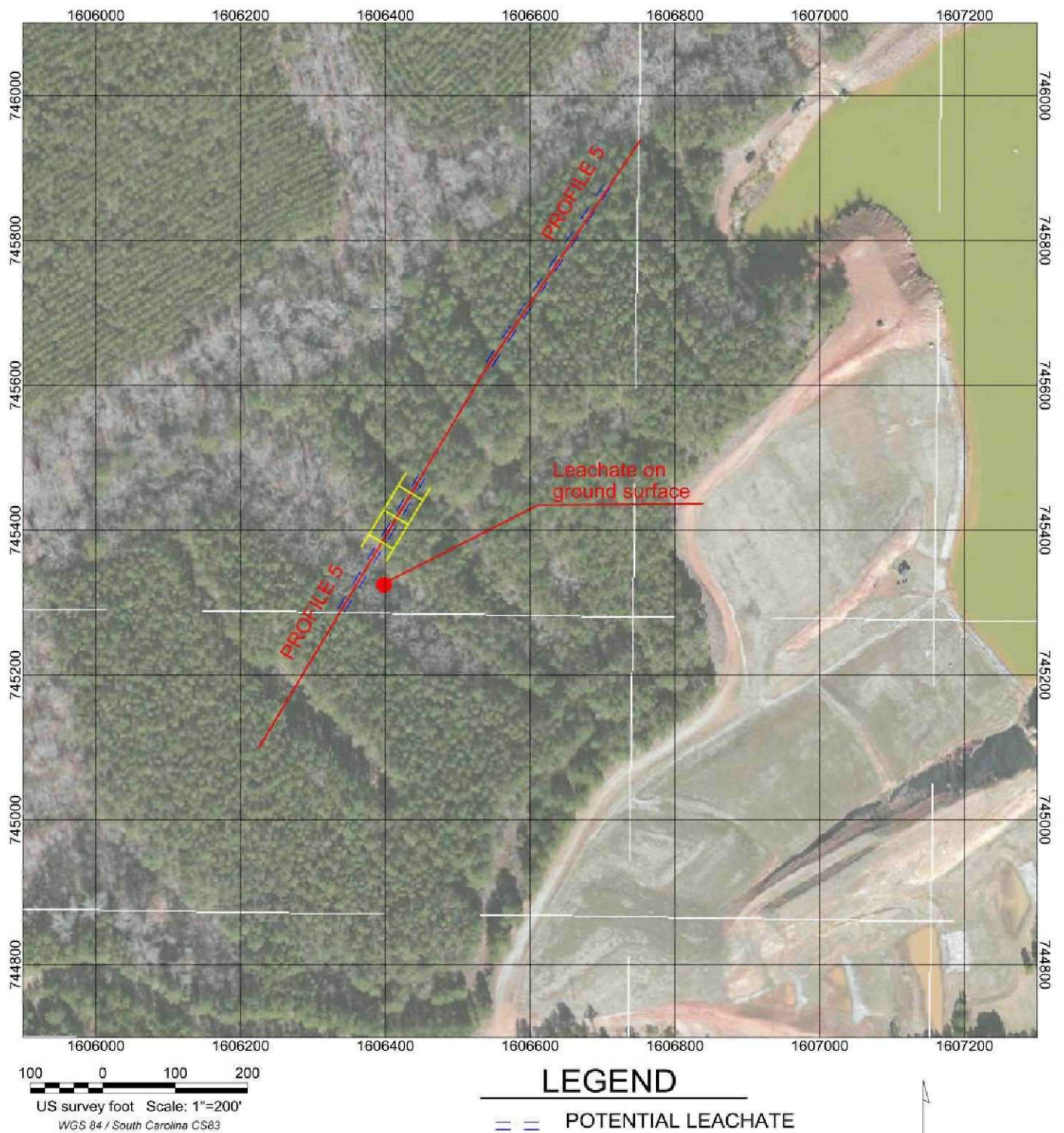
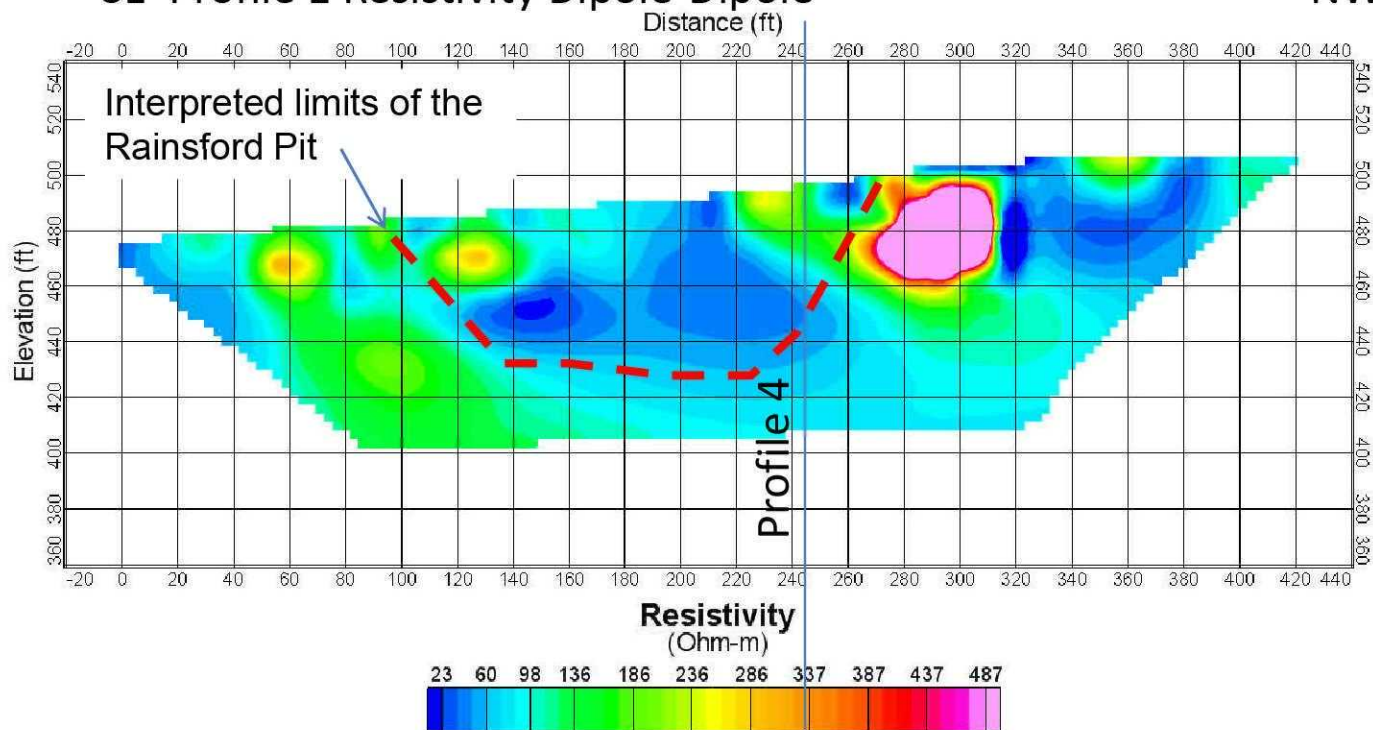


FIGURE 3 ERI INTERPRETATIONS FOR PROFILE 5

APPENDIX 1
INVERTED ERI PROFILES

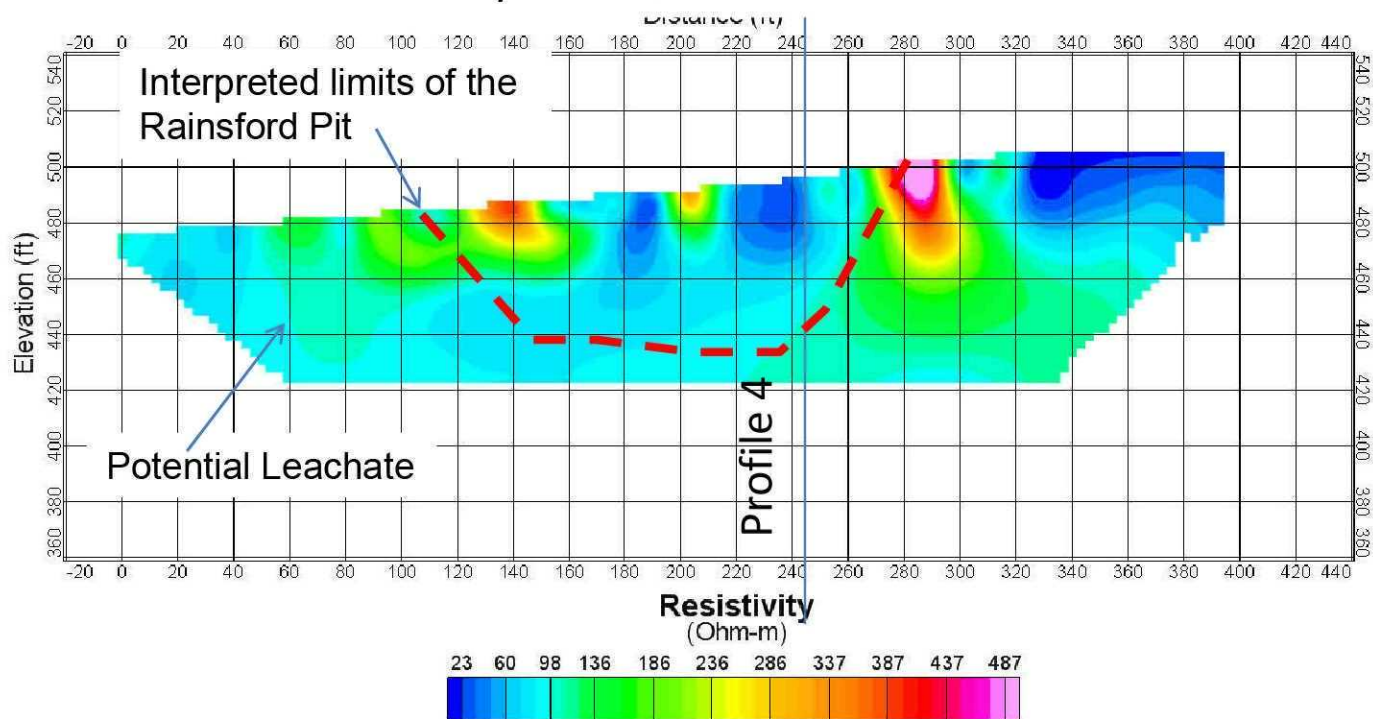
SE Profile 1 Resistivity Dipole-Dipole

NW



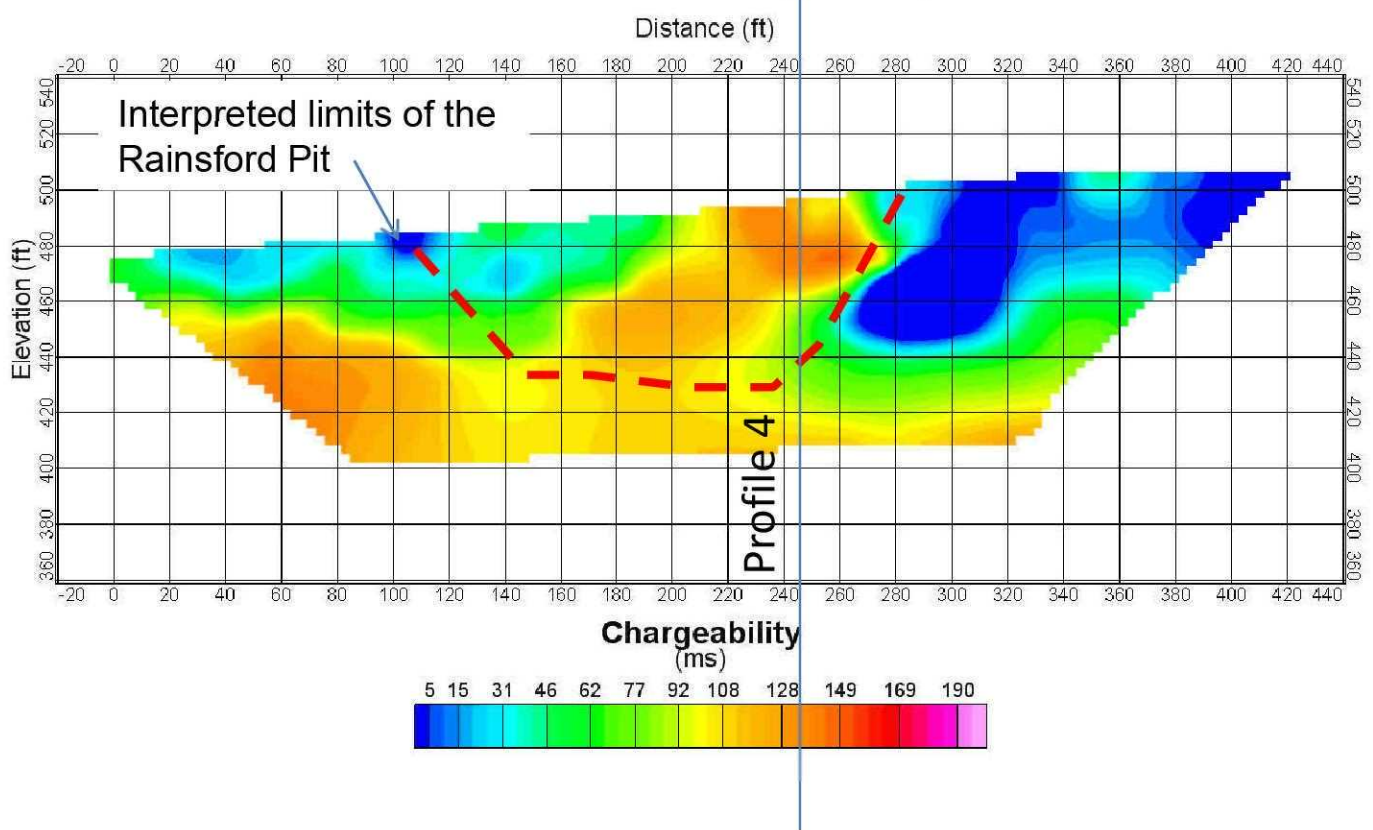
SE Profile 1 Resistivity Wenner

NW



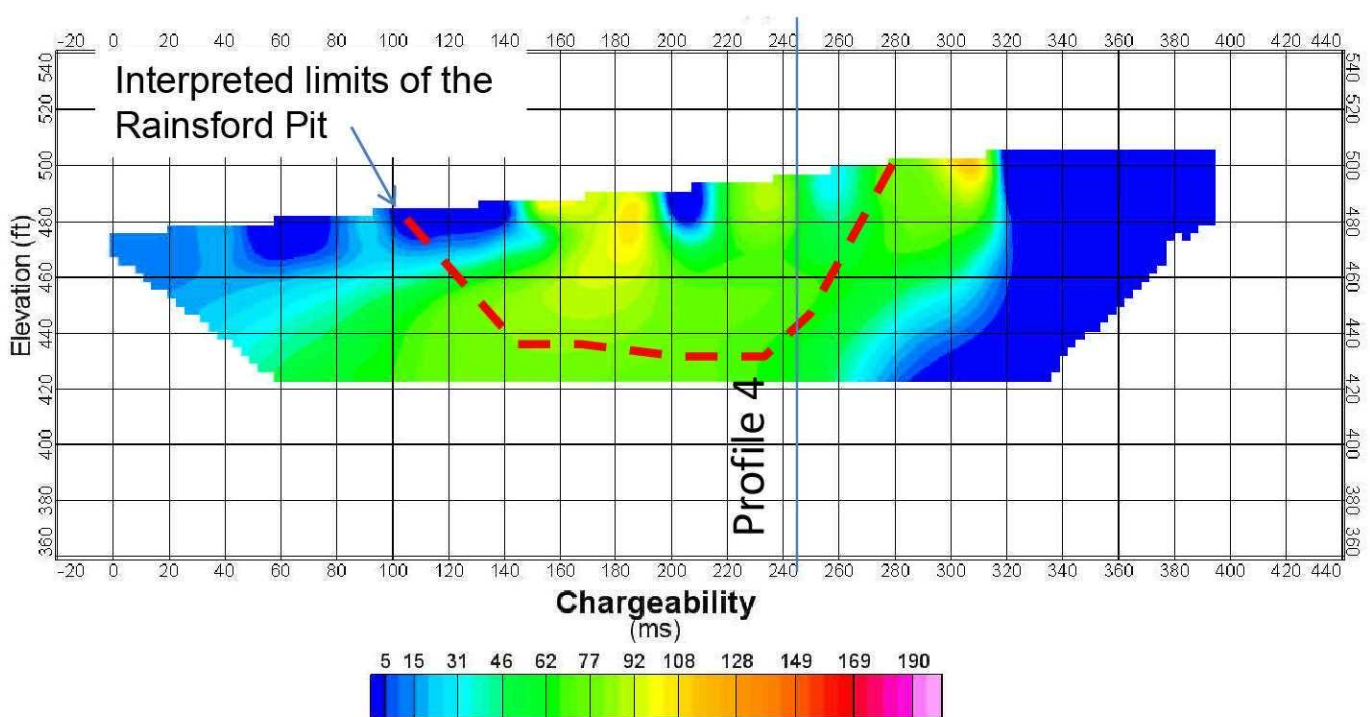
SE Profile 1 Induced Polarization Dipole-Dipole

NW



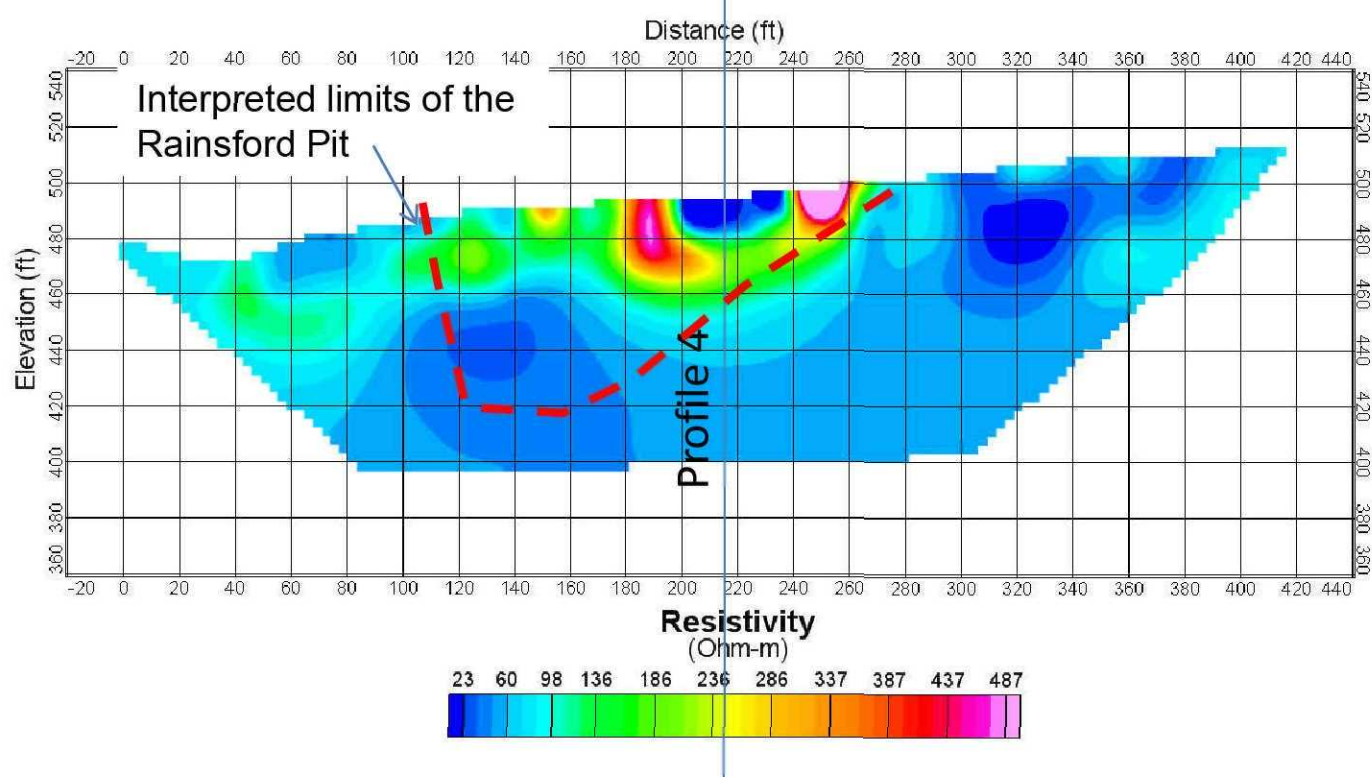
SE Profile 1 – Induced Polarization Wenner

NW



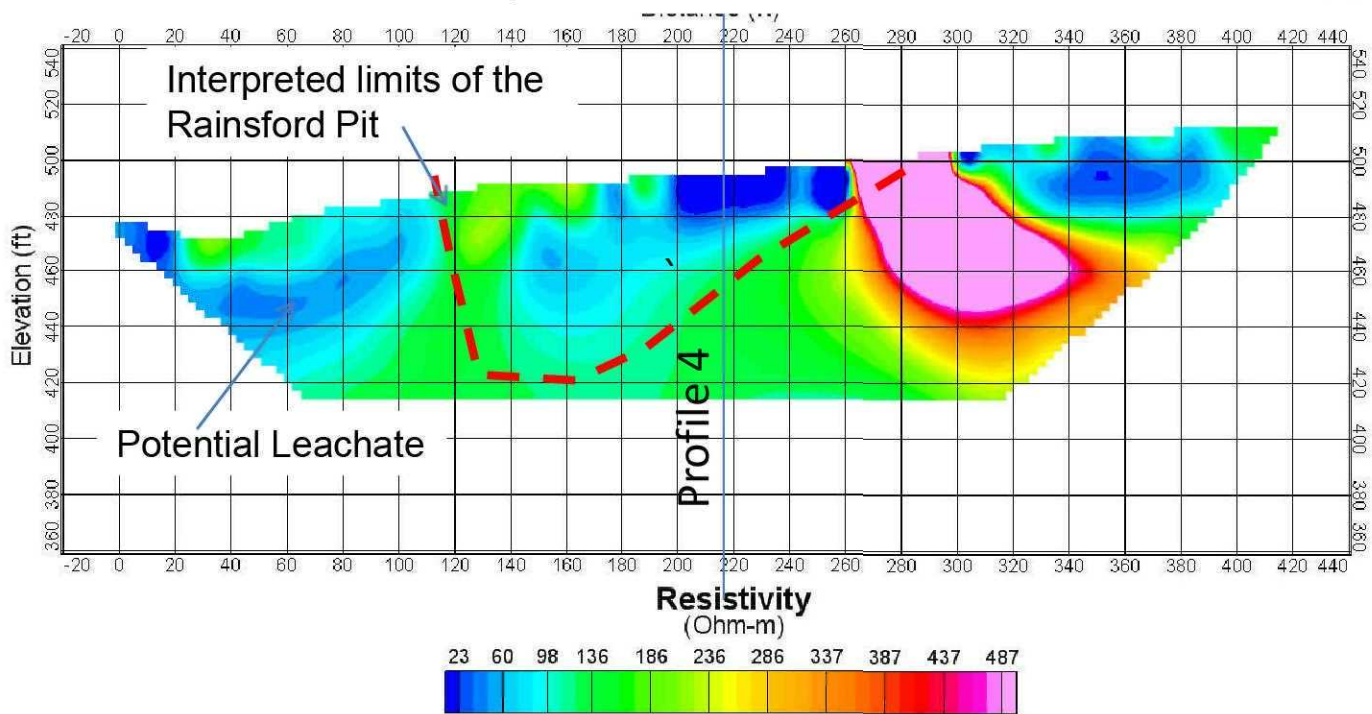
SE Profile 2, Resistivity Dipole-Dipole

NW



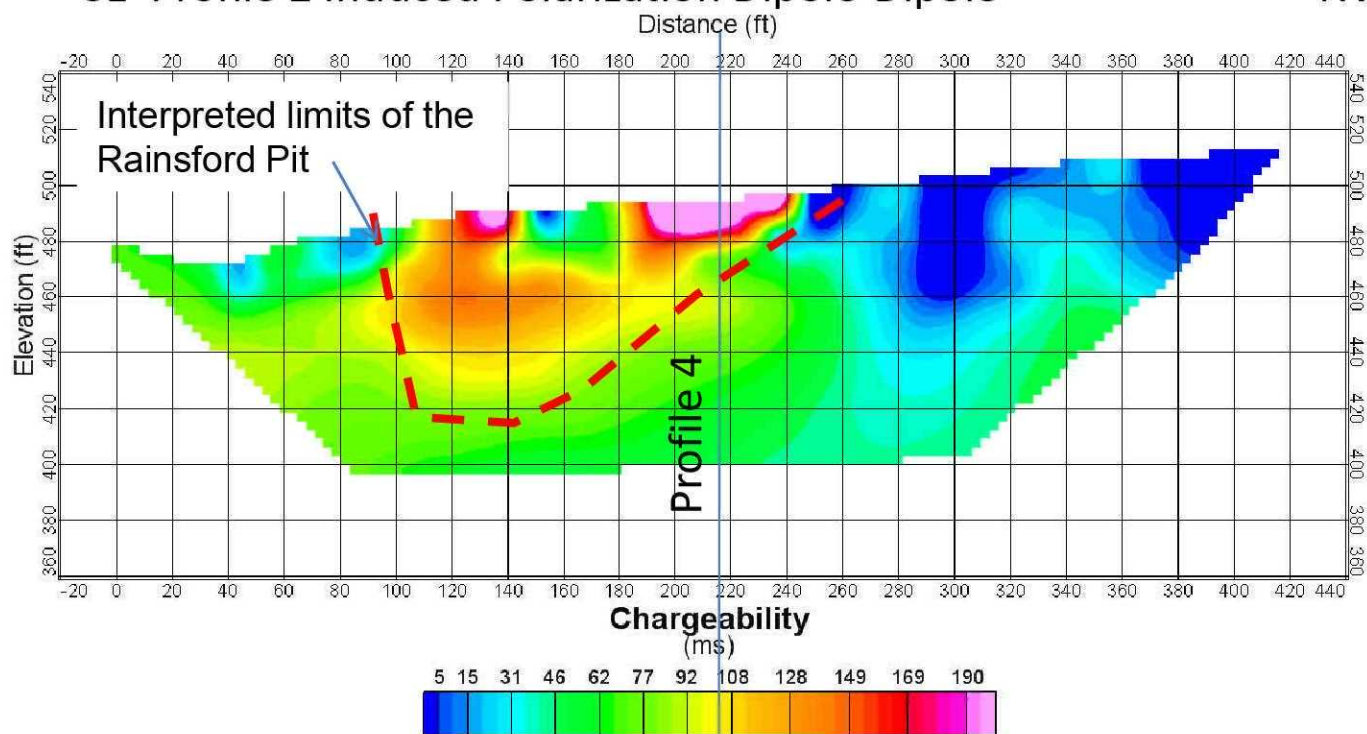
SE Profile 2 Resistivity Wenner

NW



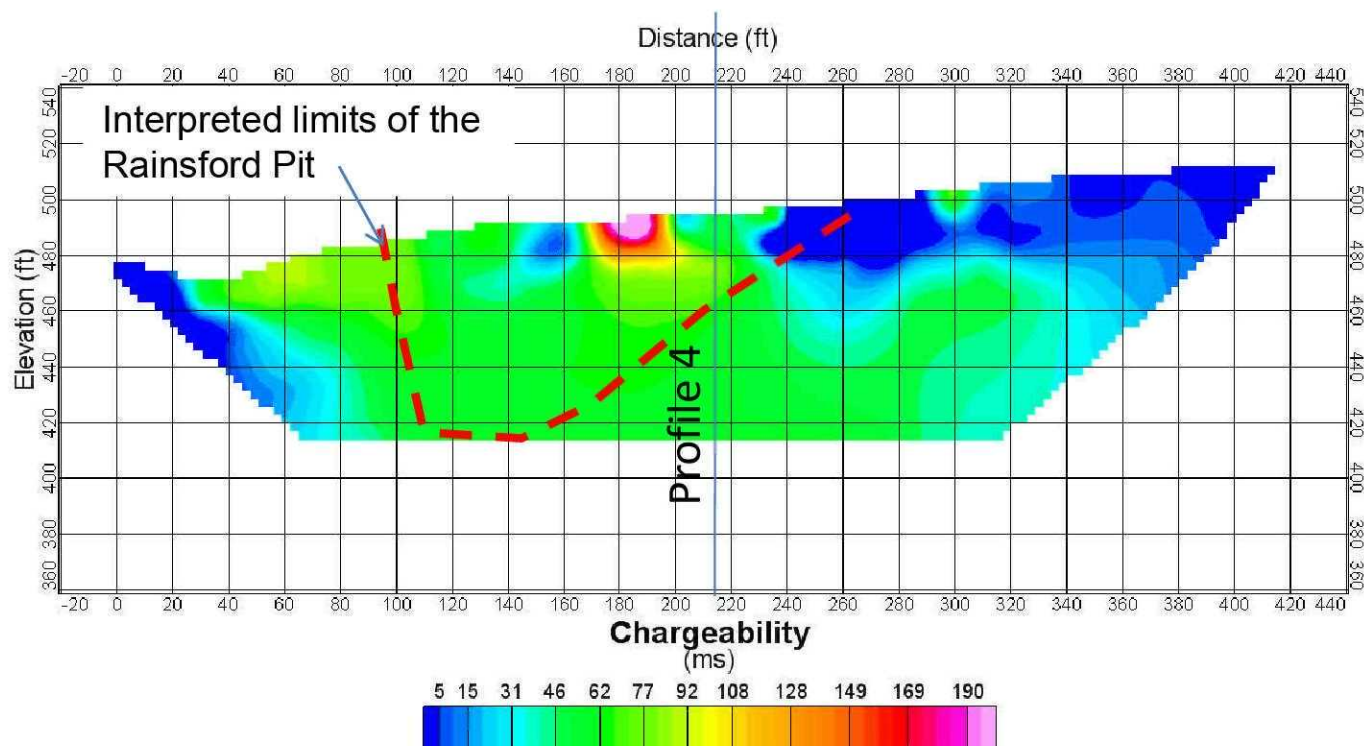
SE Profile 2 Induced Polarization Dipole-Dipole

NW



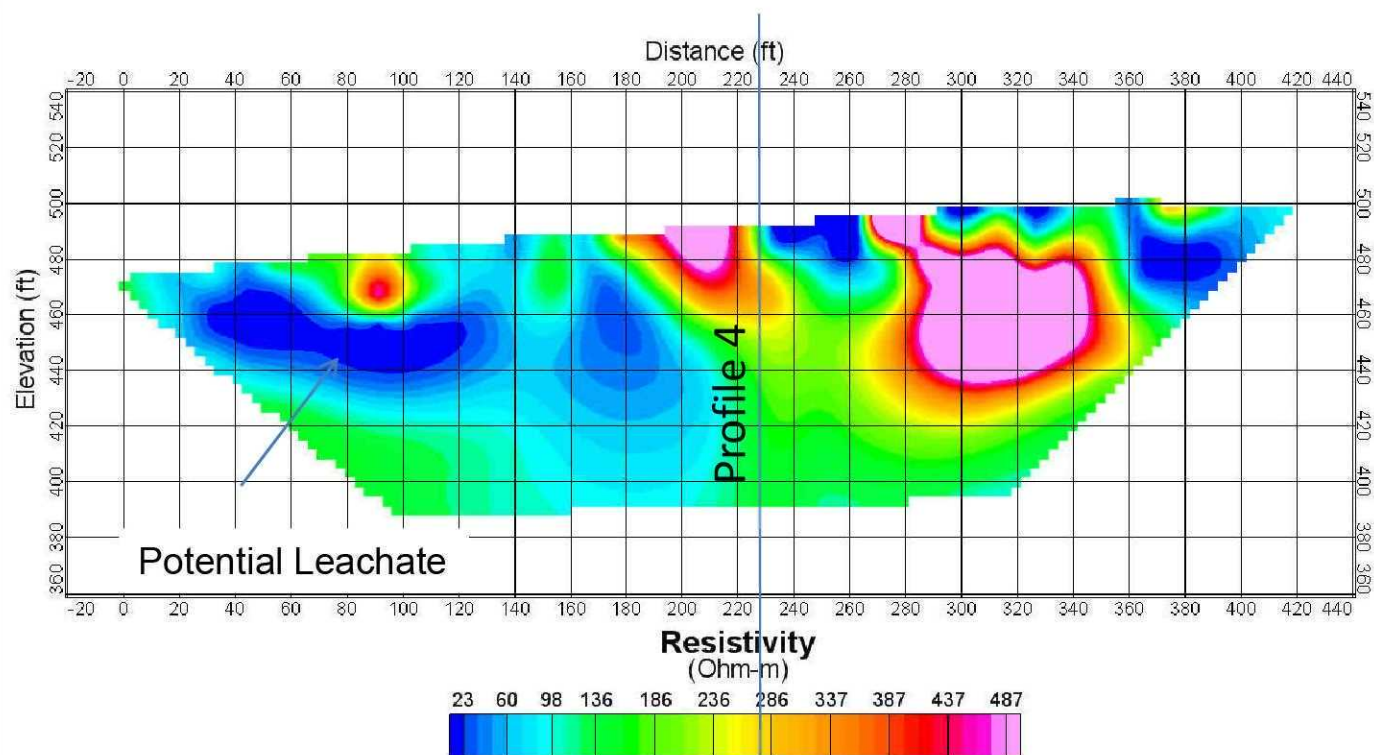
SE Profile 2- Induced Polarization Wenner

NW



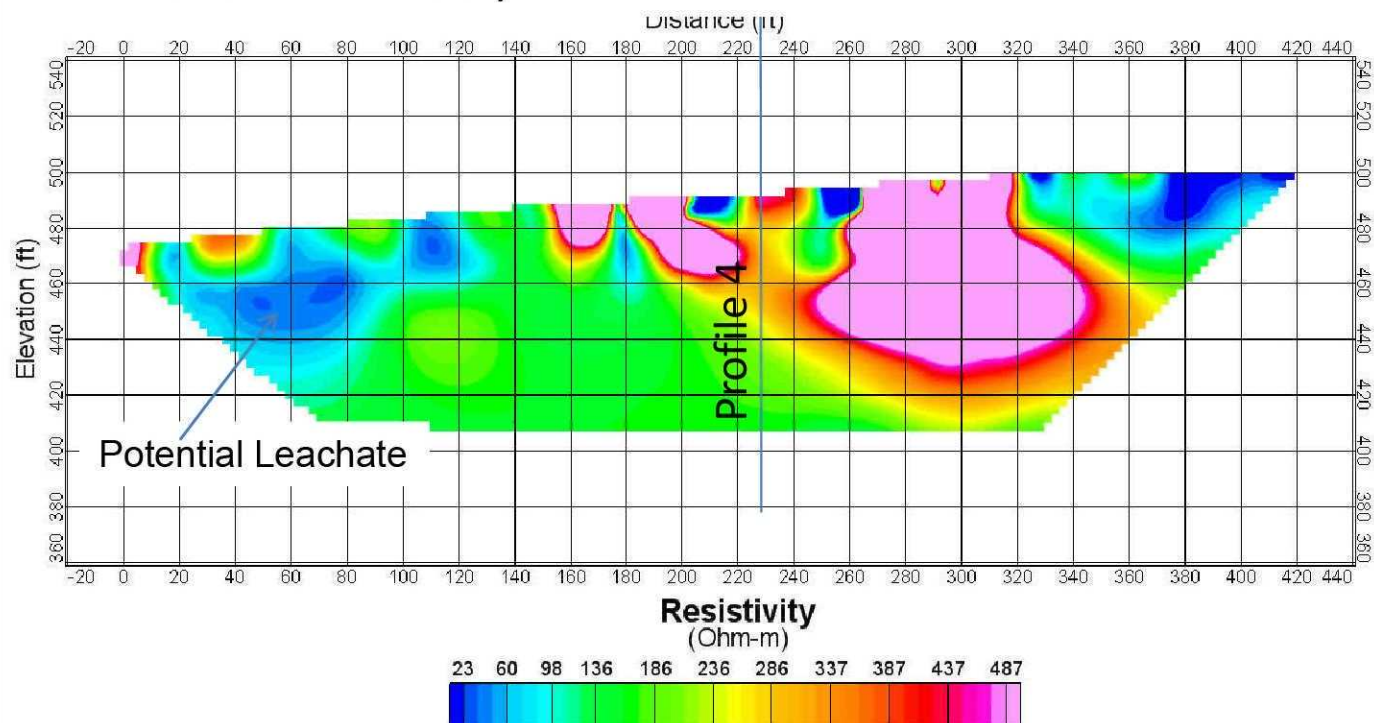
SE Profile 3 Resistivity Dipole-Dipole

NW



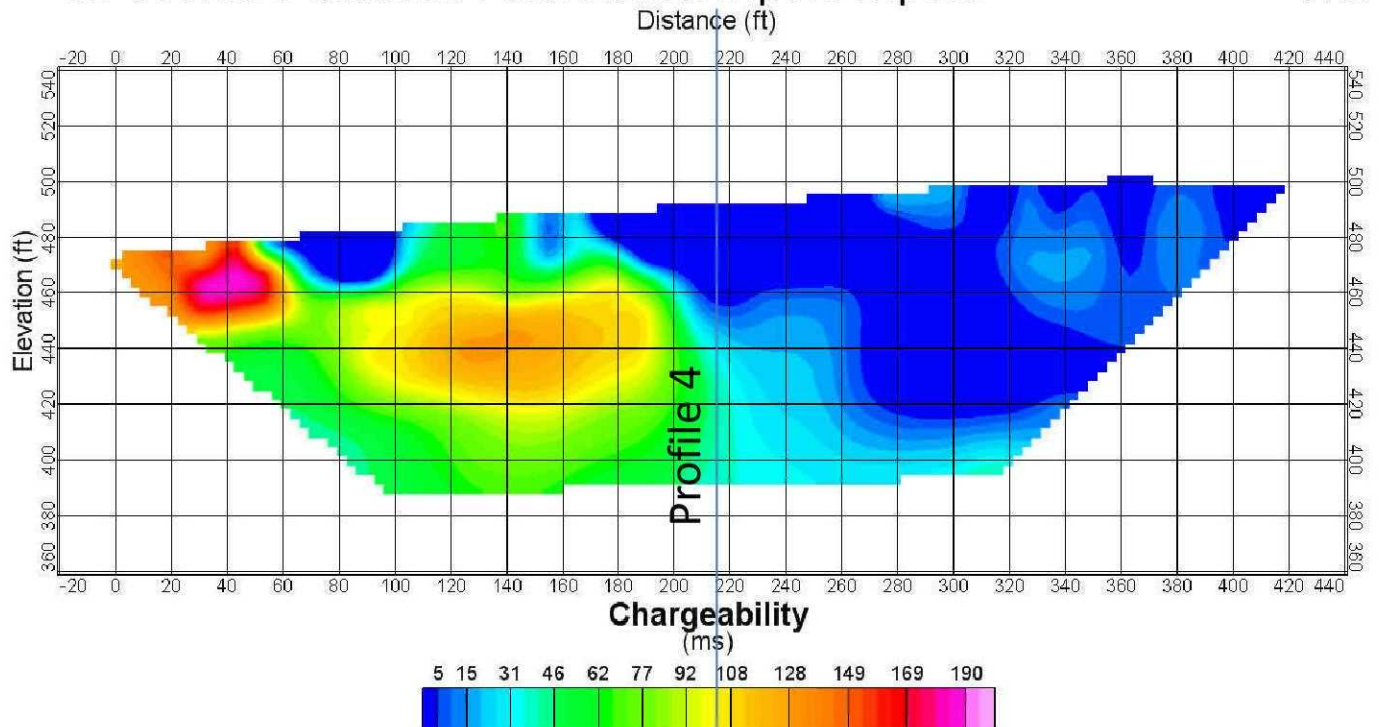
SE Profile 3 Resistivity Wenner

NW



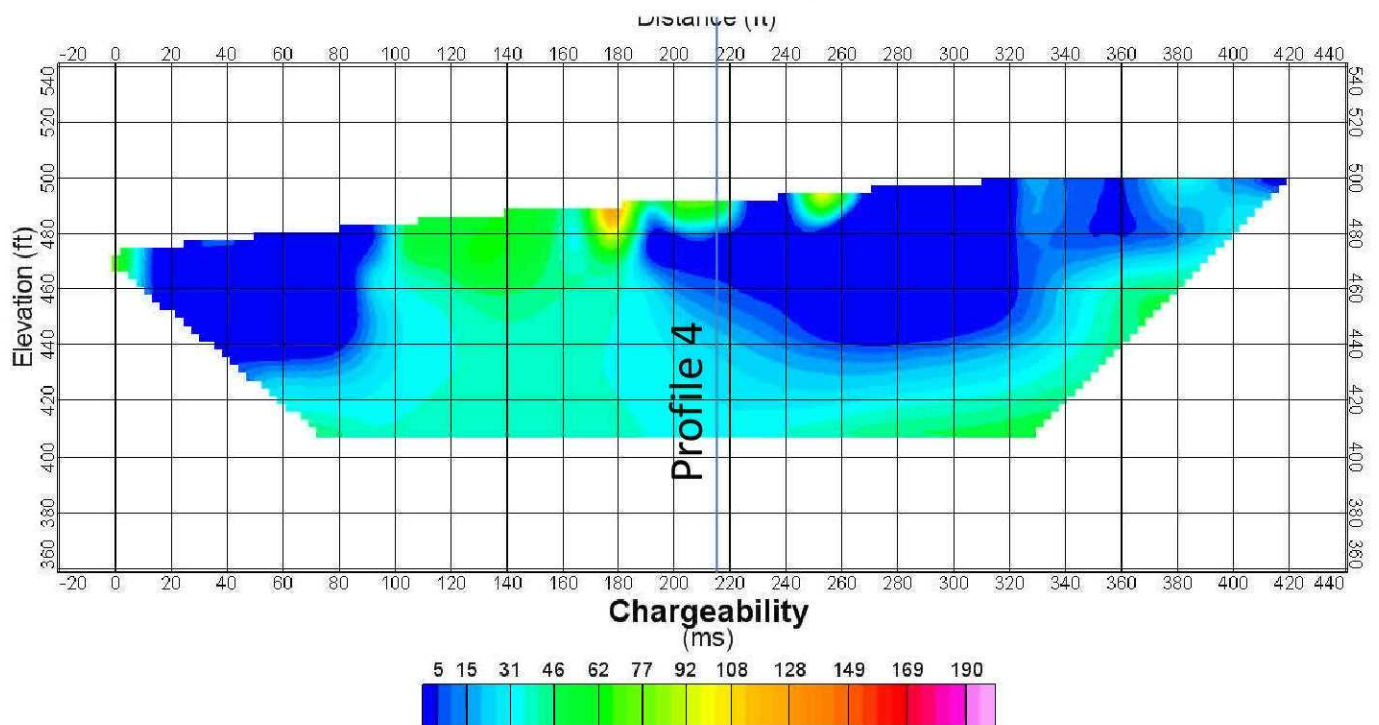
SE Profile 3 Induced Polarization Dipole-Dipole

NW



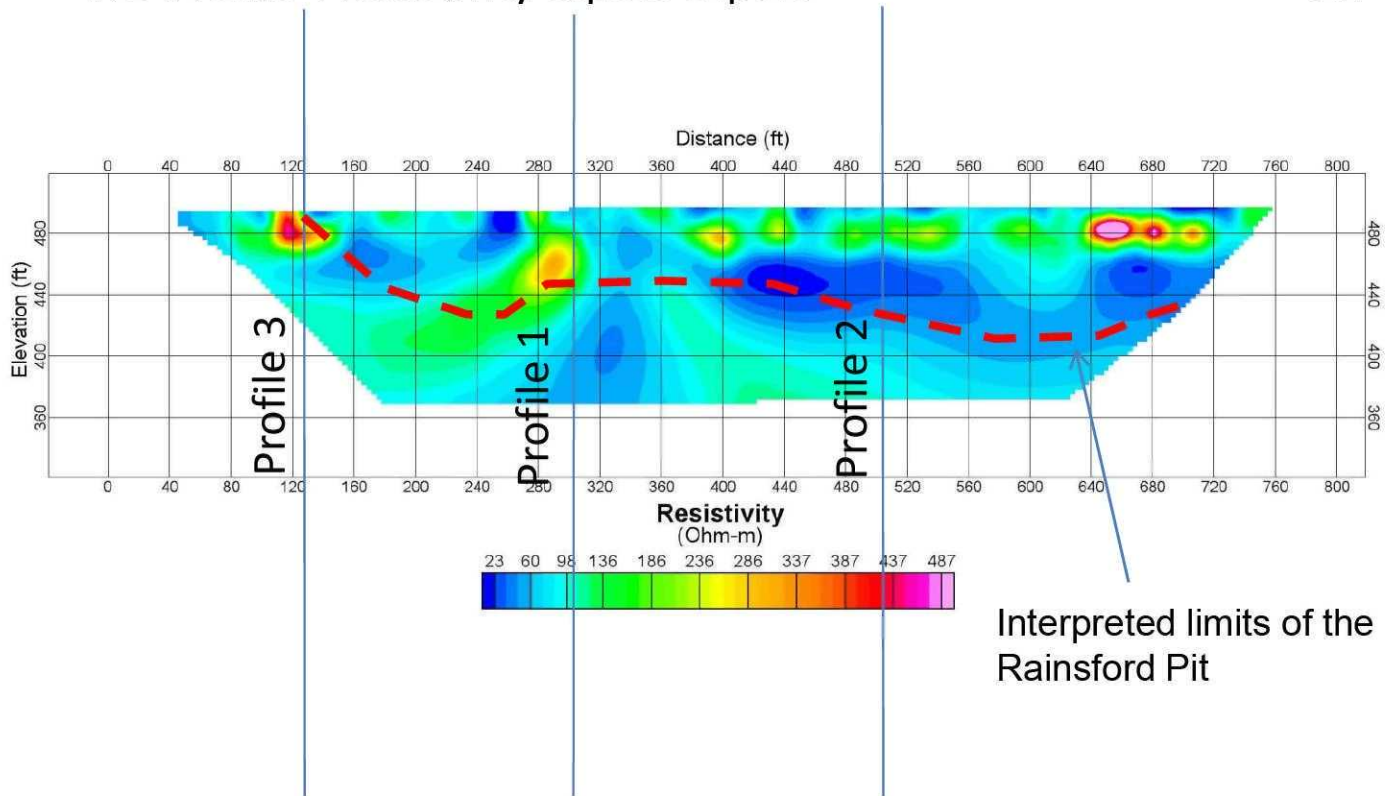
SE Profile 3- Induced Polarization Wenner

NW



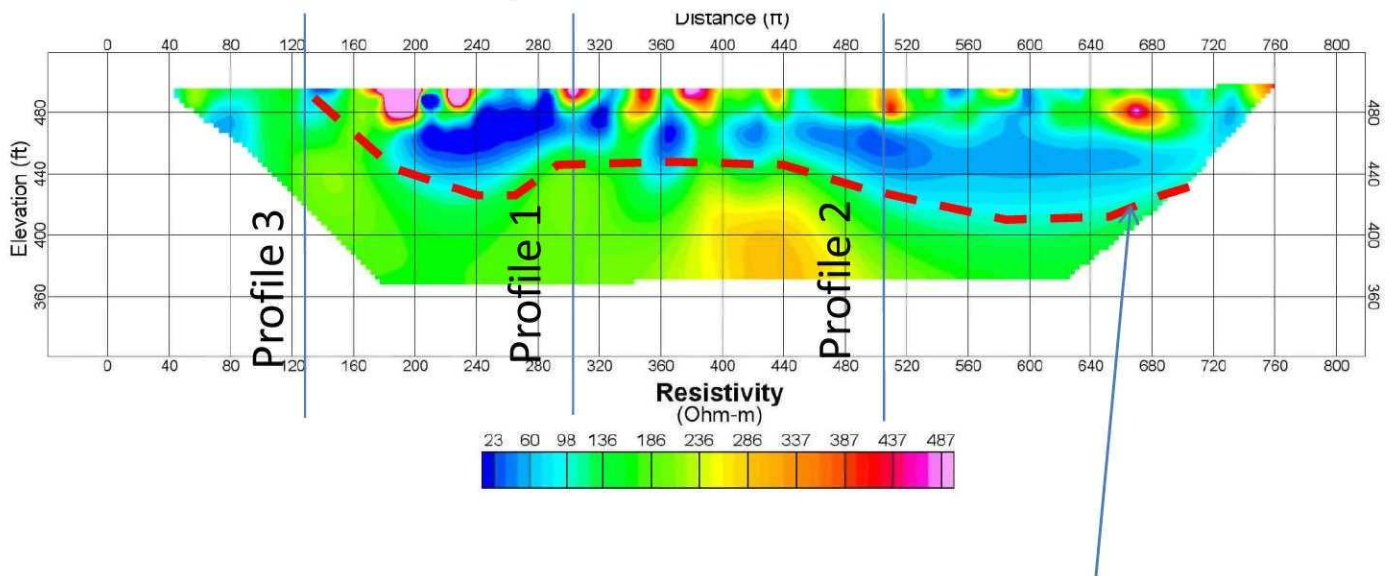
NE Profile 4 Resistivity Dipole-Dipole

SW



NE Profile 4 Resistivity Wenner

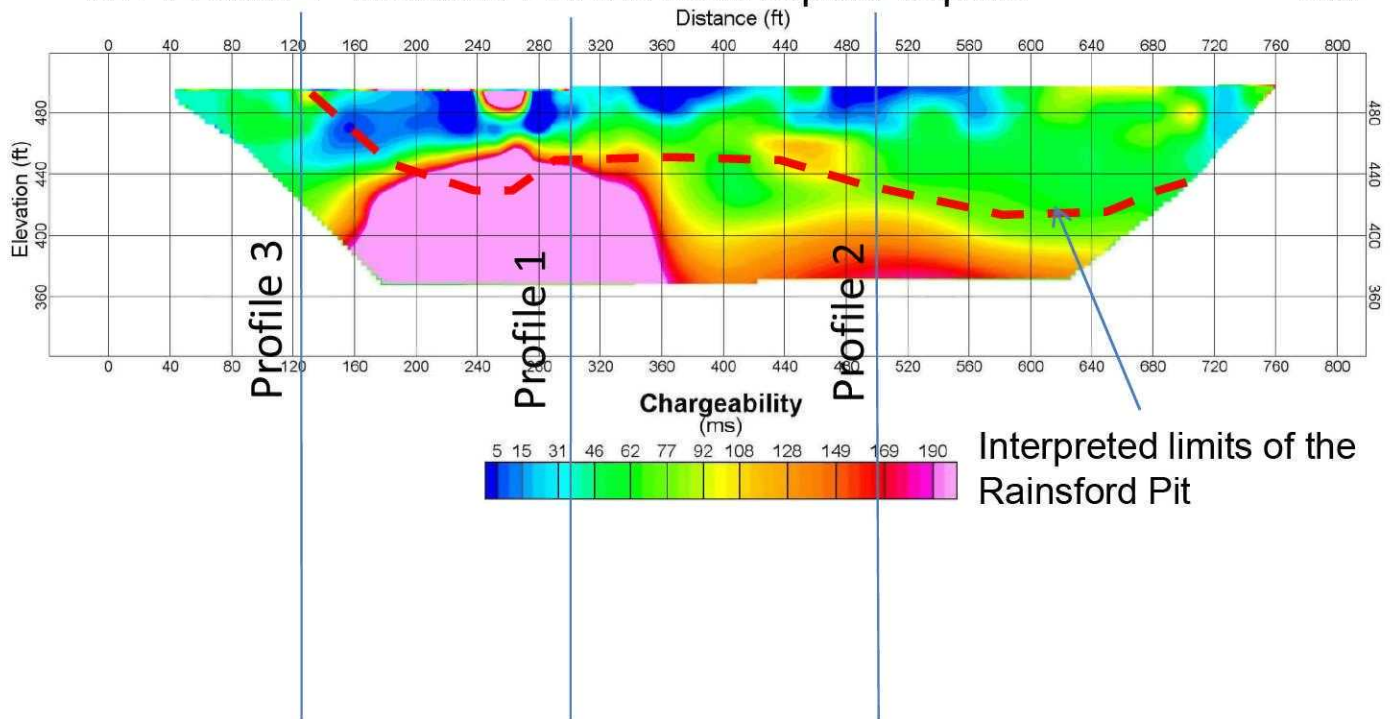
SW



Interpreted limits of the
Rainsford Pit

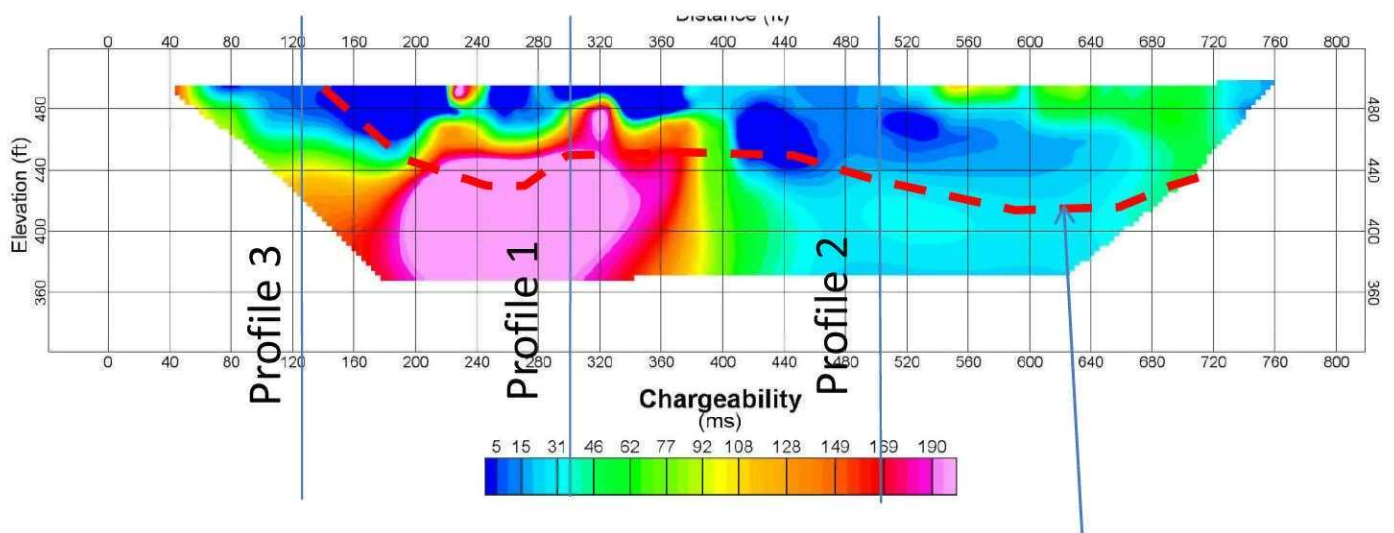
NE Profile 4- Induced Polarization Dipole-Dipole

SW



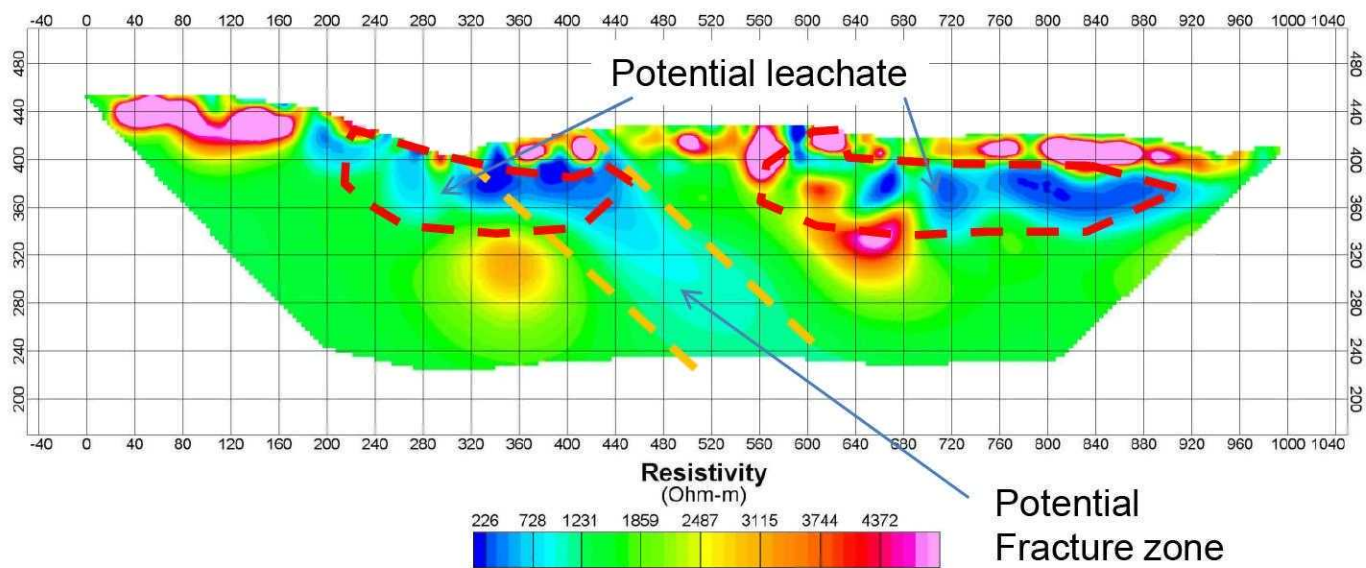
NE Profile 4- Induced Polarization Wenner

SW



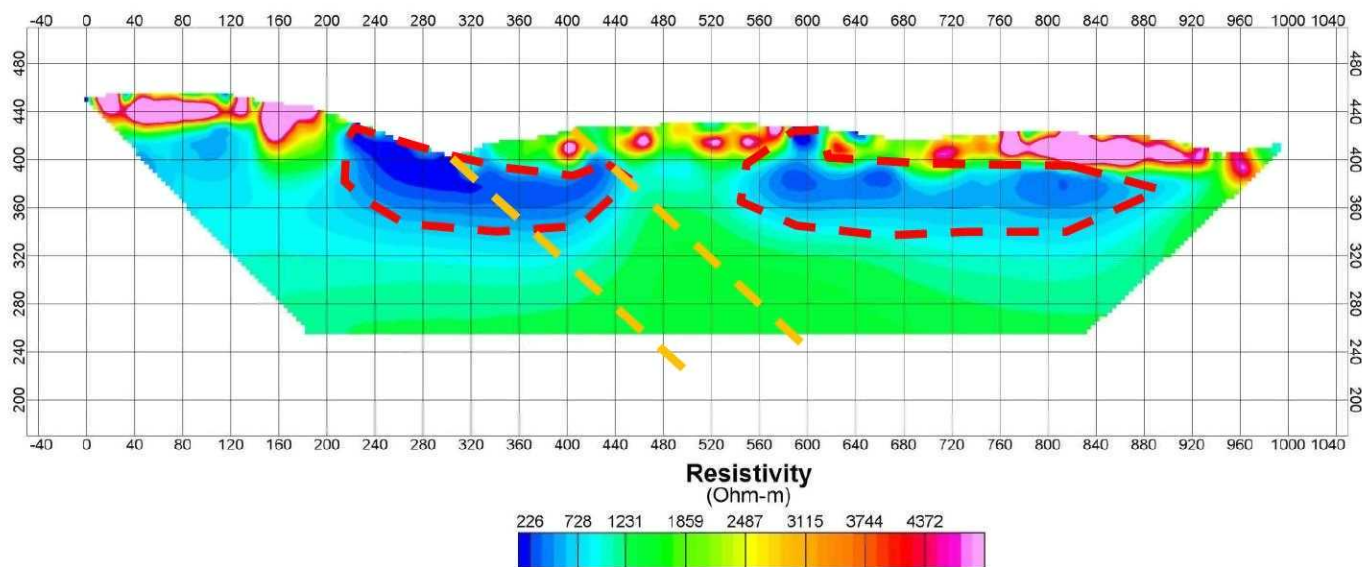
SW Profile 5 Resistivity Dipole-Dipole

NE



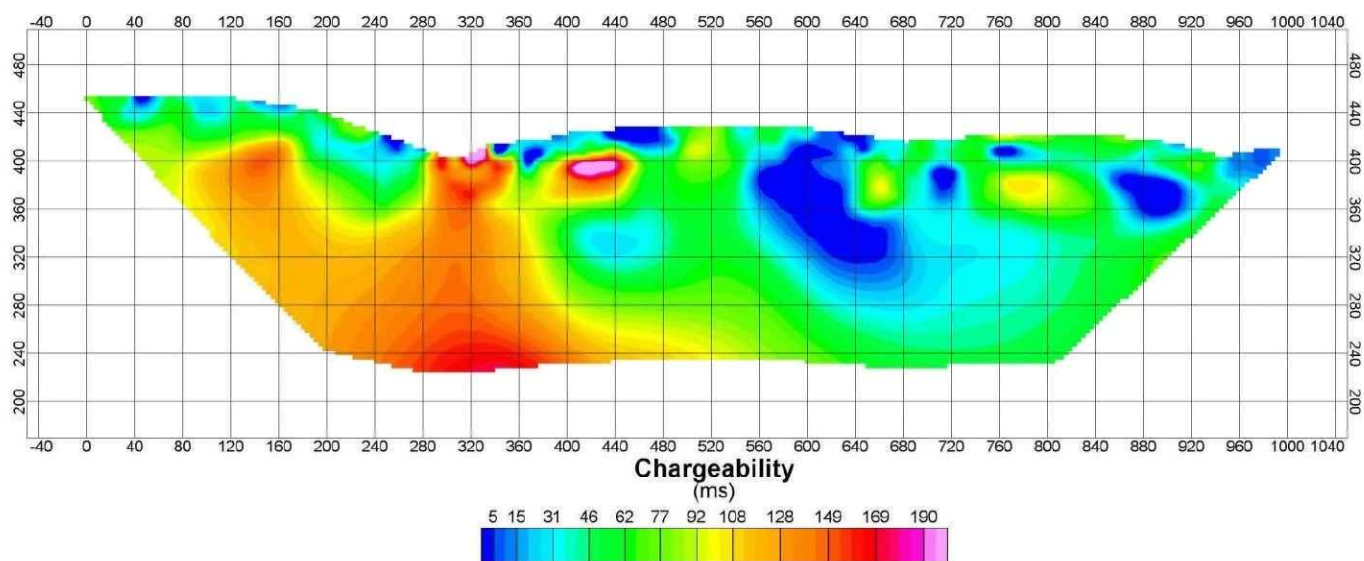
SW Profile 5 Resistivity Wenner

NE



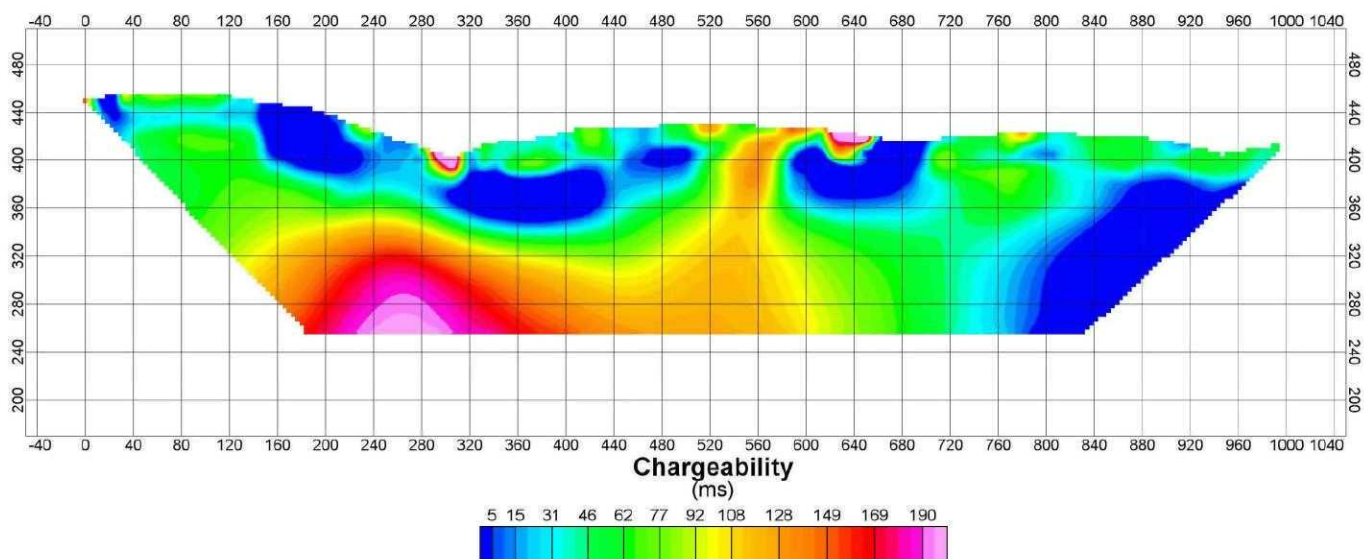
SW Profile 5- Induced Polarization Dipole-Dipole

NE



SW Profile 5- Induced Polarization Wenner

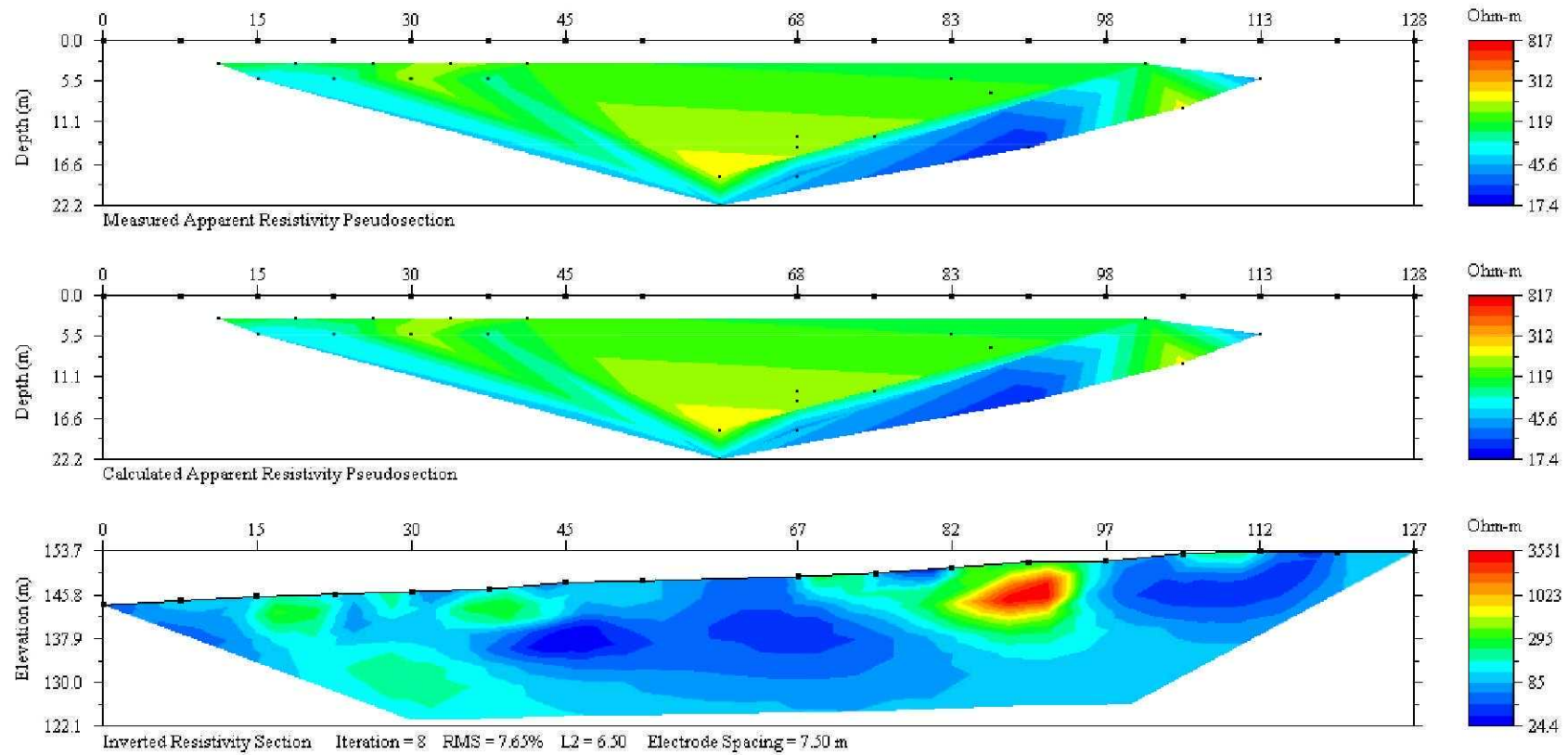
NE



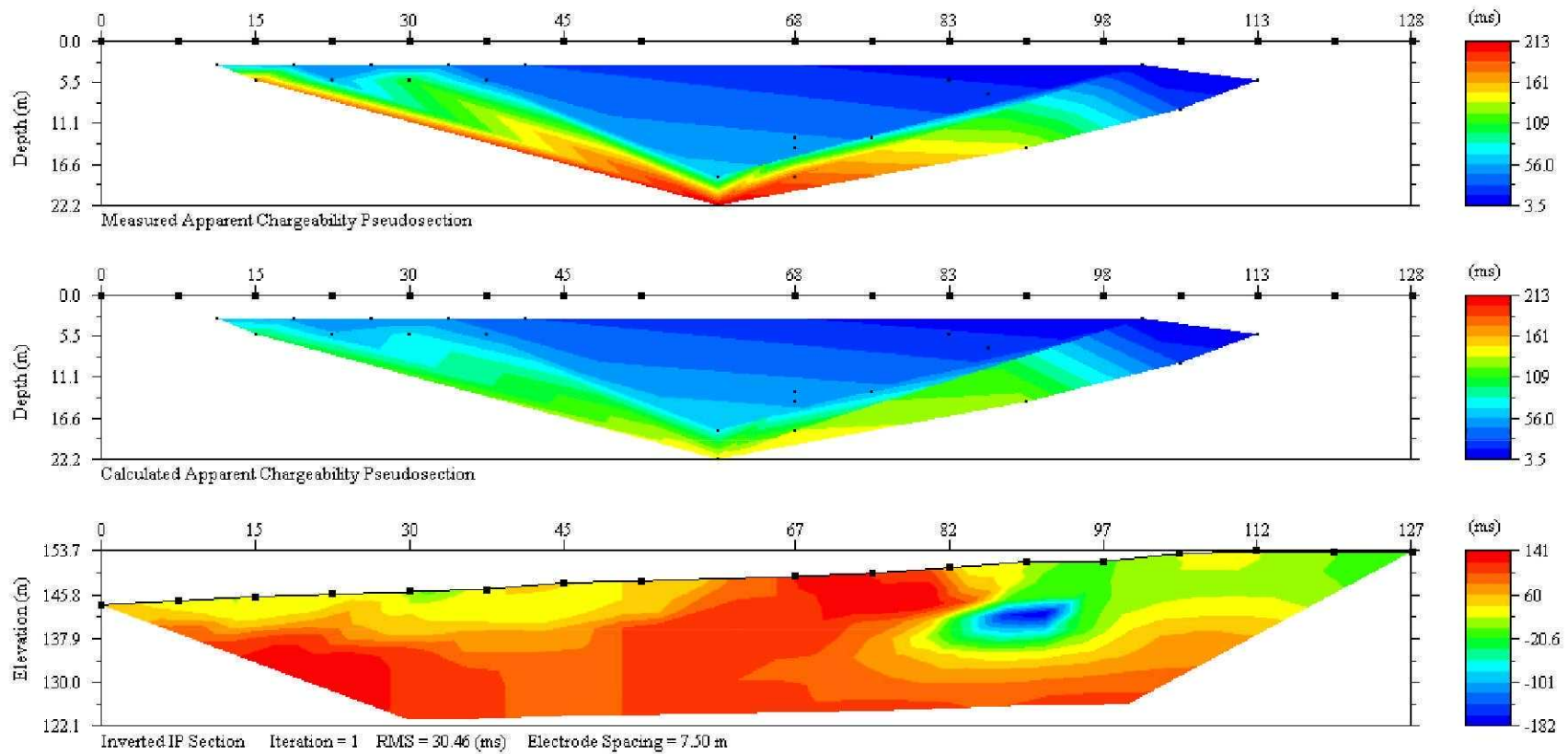
APPENDIX 2

RAW DATA, CALCULATED DATA AND ERI MODELS

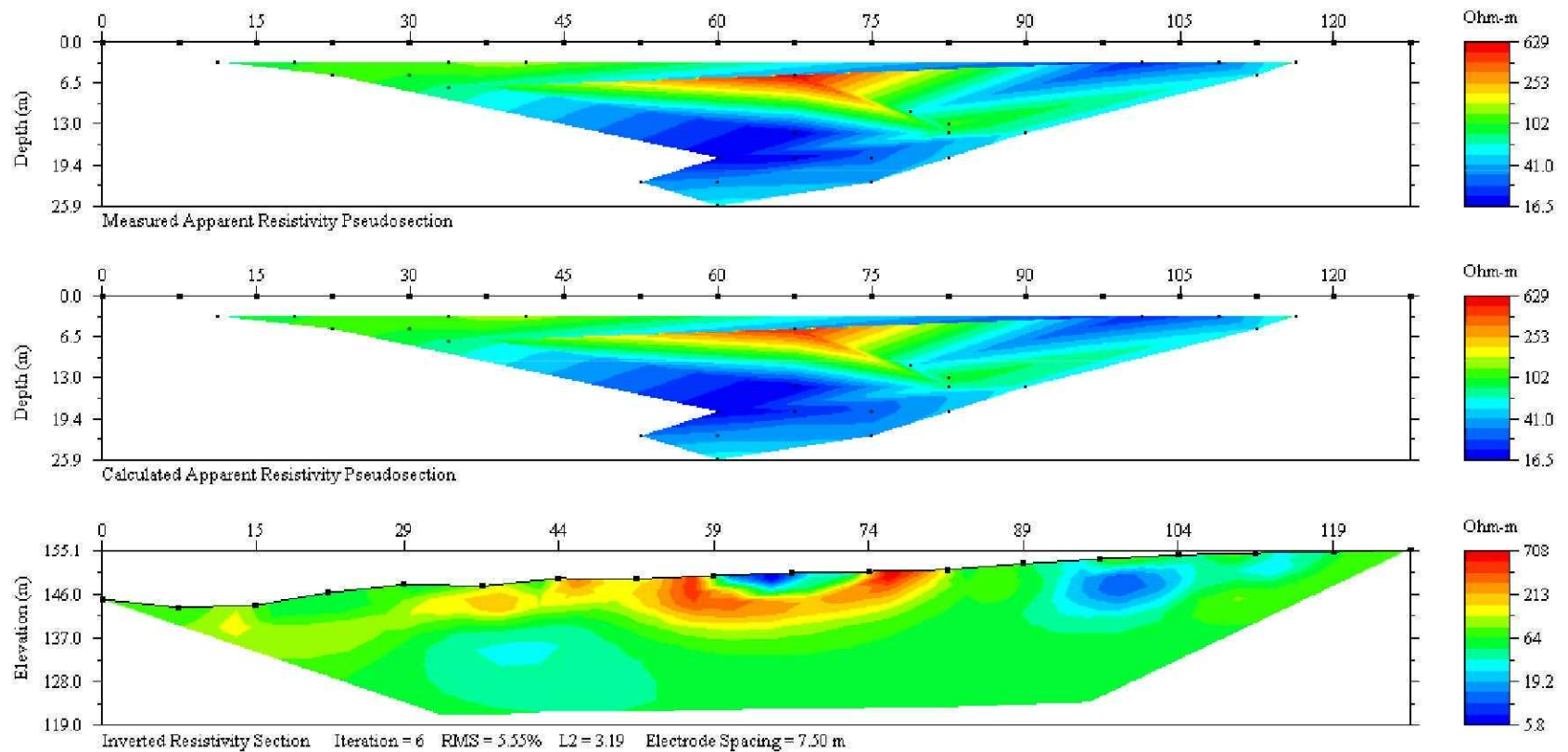
Profile 1 Resistivity Dipole-Dipole



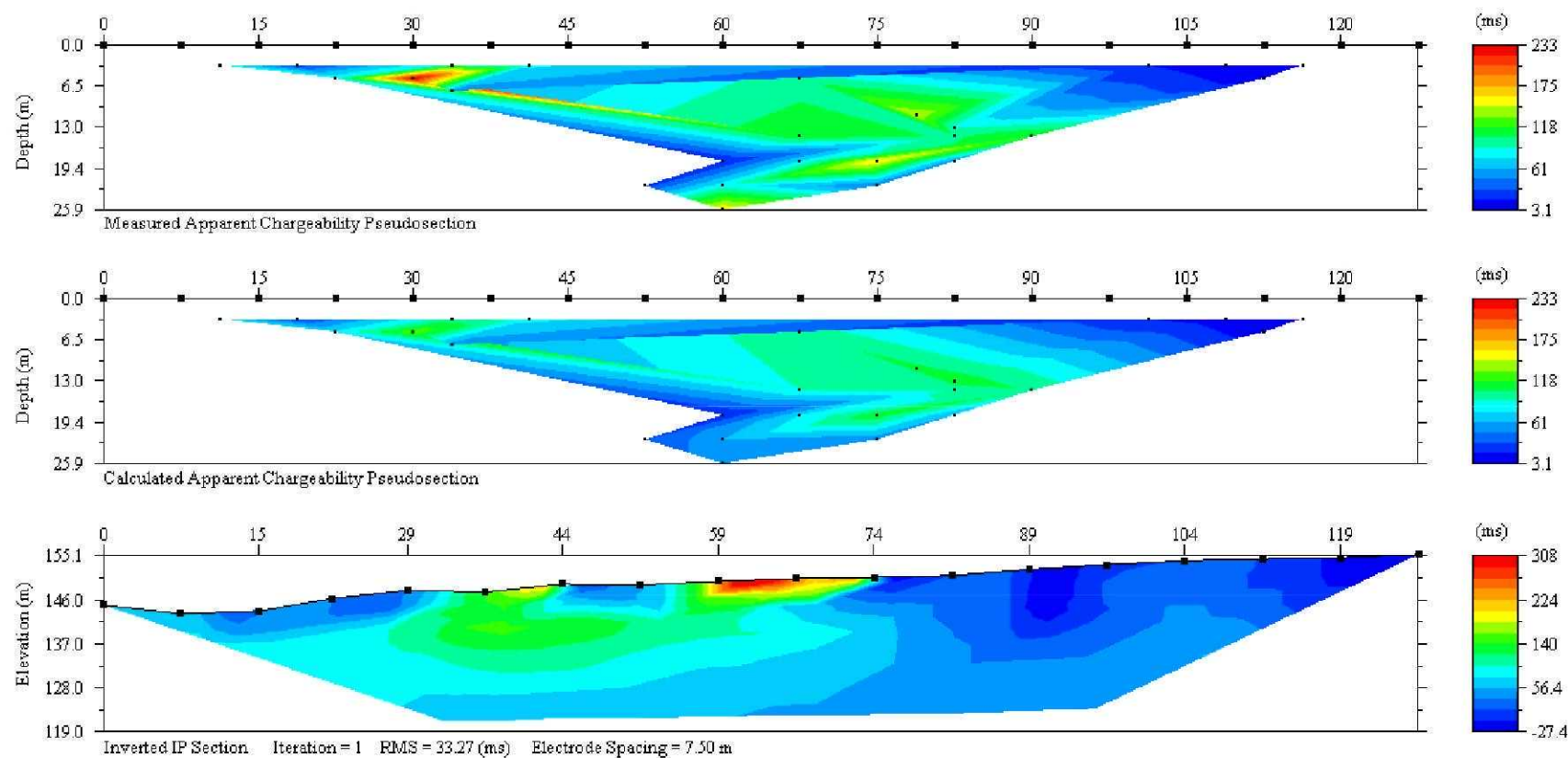
Profile 1 Induced Polarization Dipole-Dipole



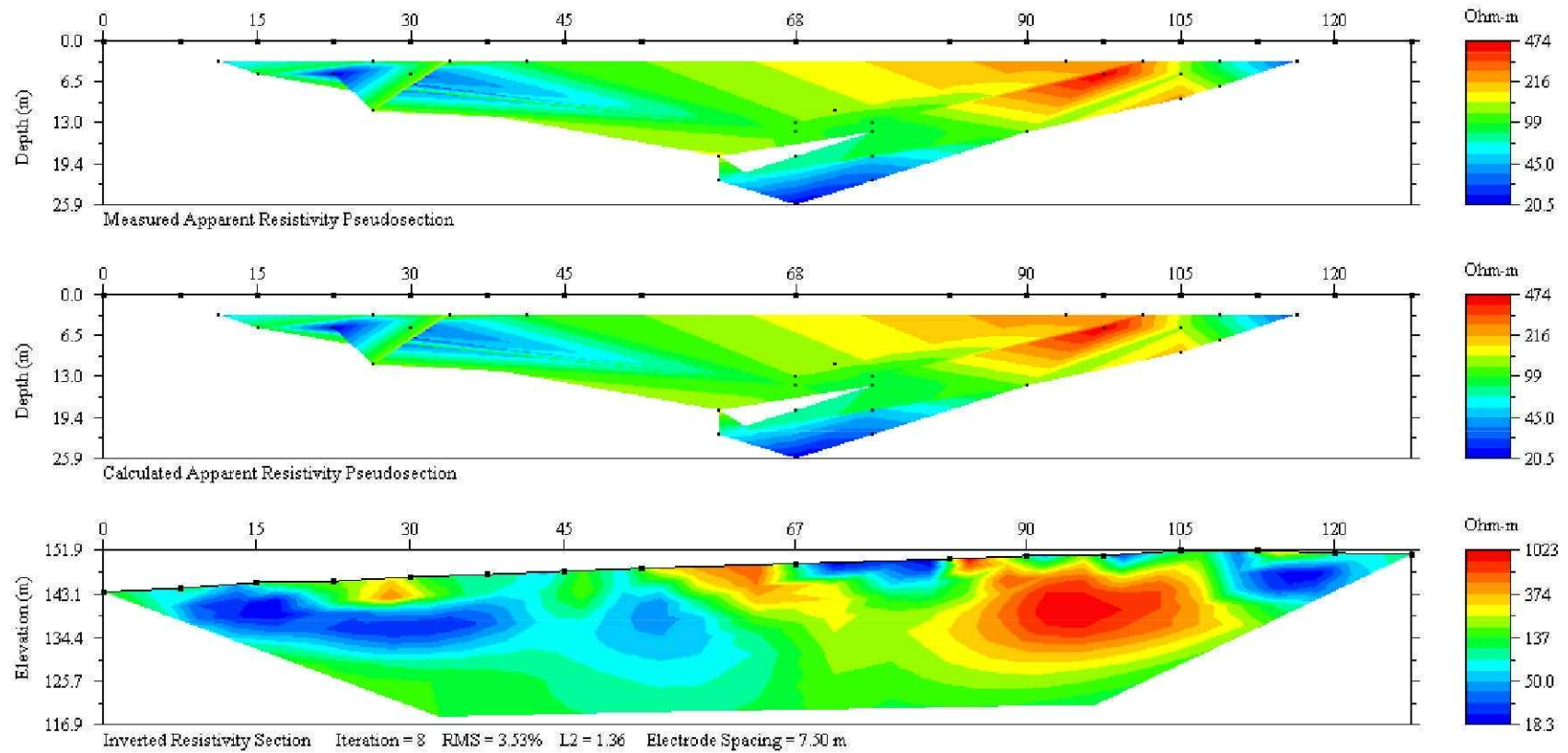
Profile 2 Resistivity Dipole-Dipole



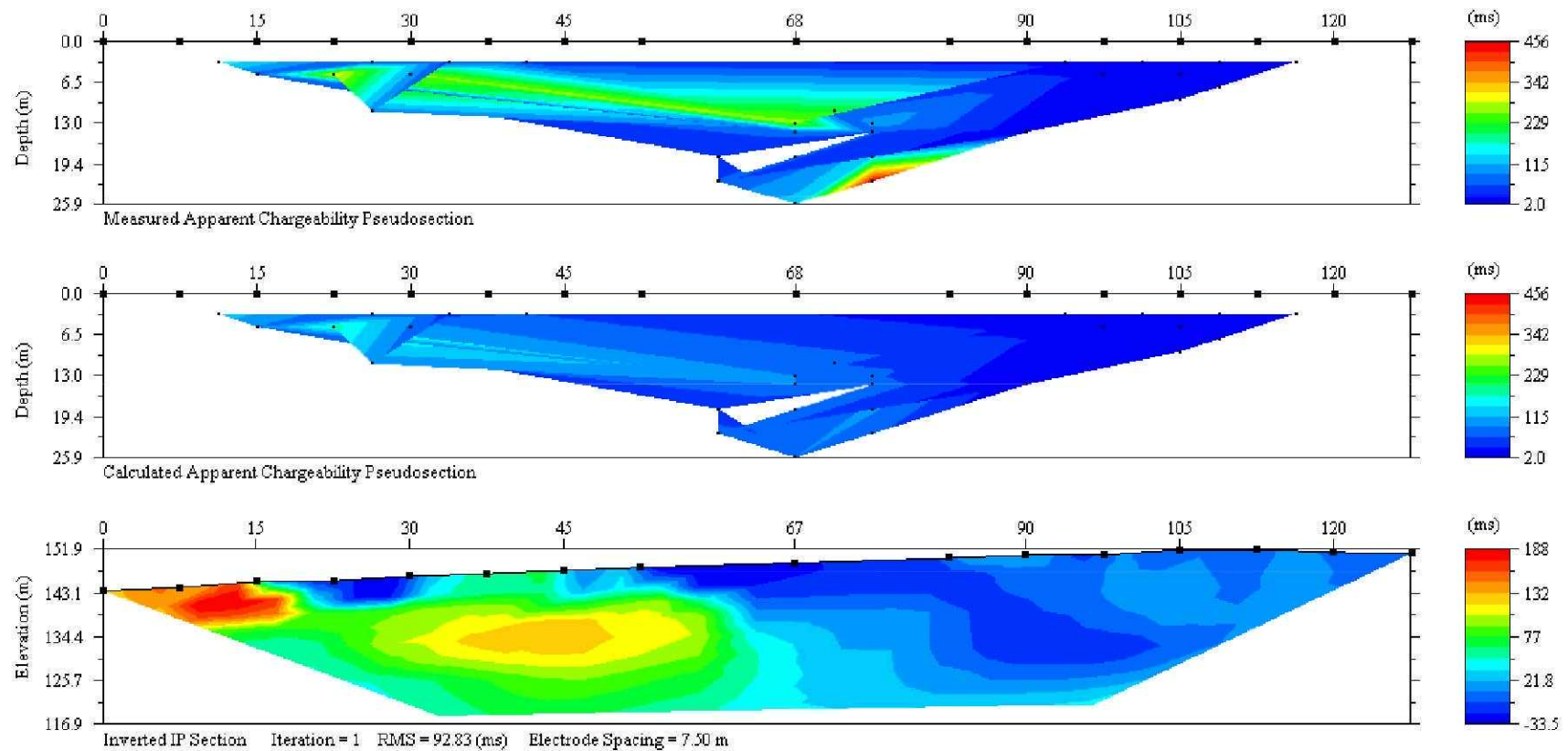
Profile 2 Induced Polarization Dipole-Dipole



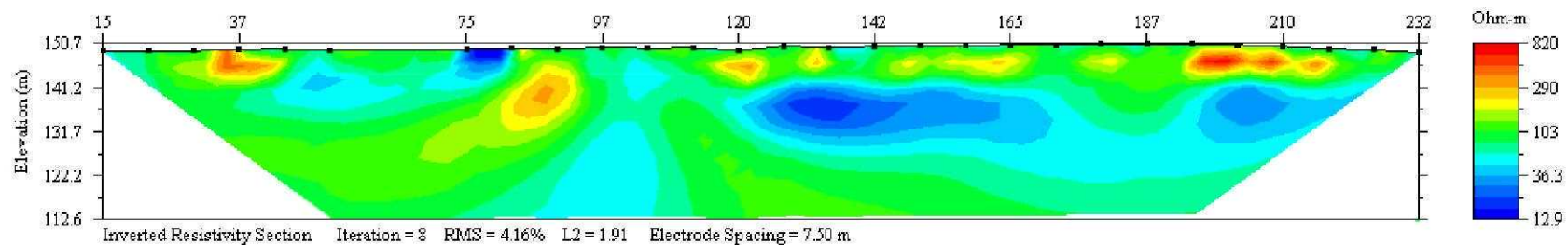
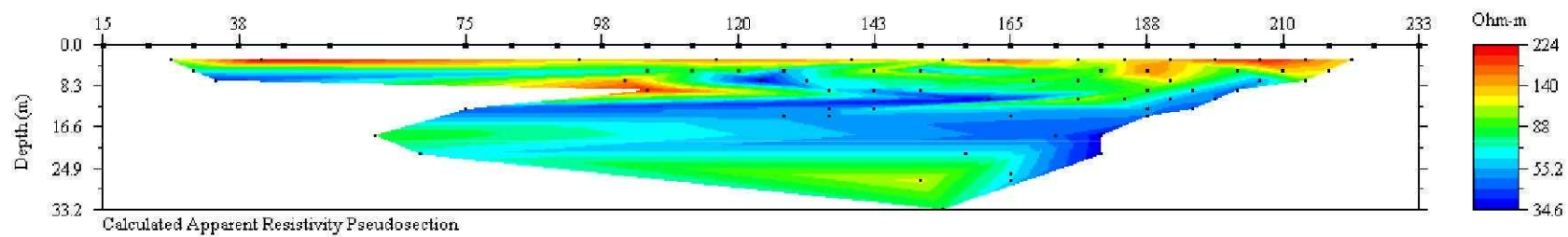
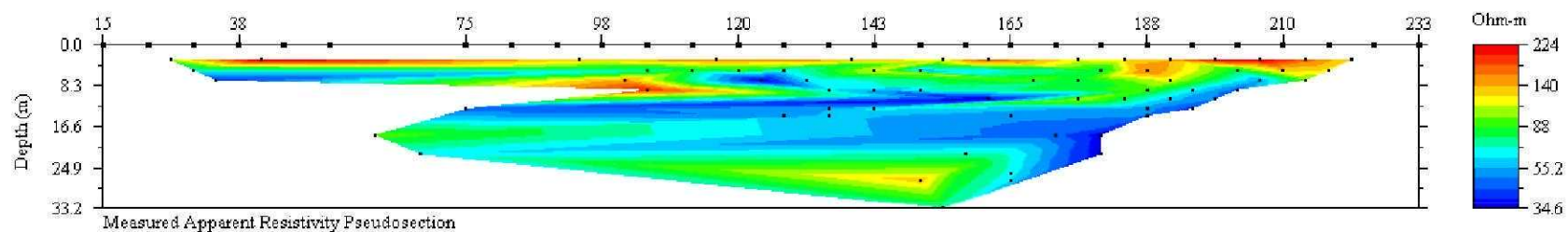
Profile 3 Resistivity Dipole-Dipole



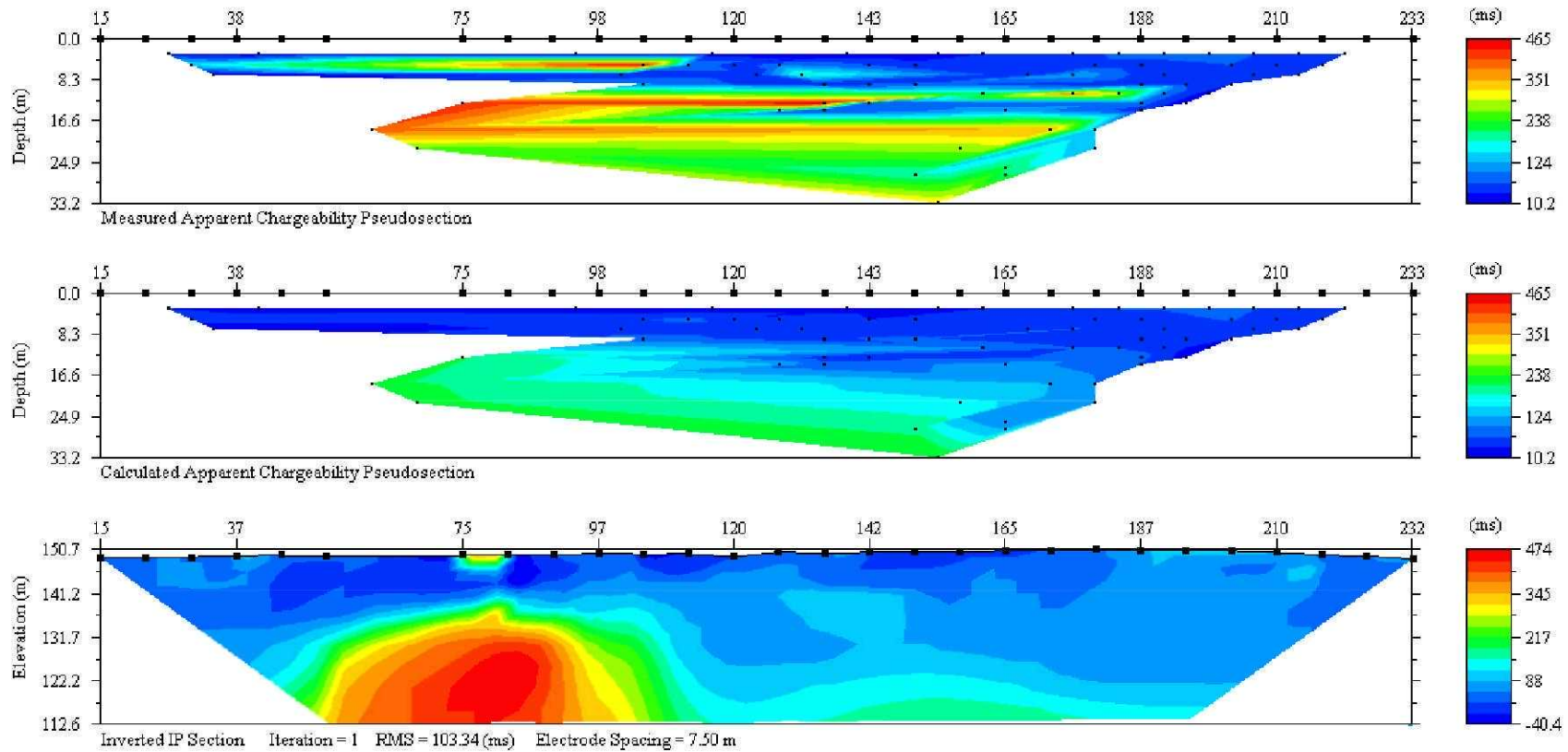
Profile 3 Induced Polarization Dipole-Dipole



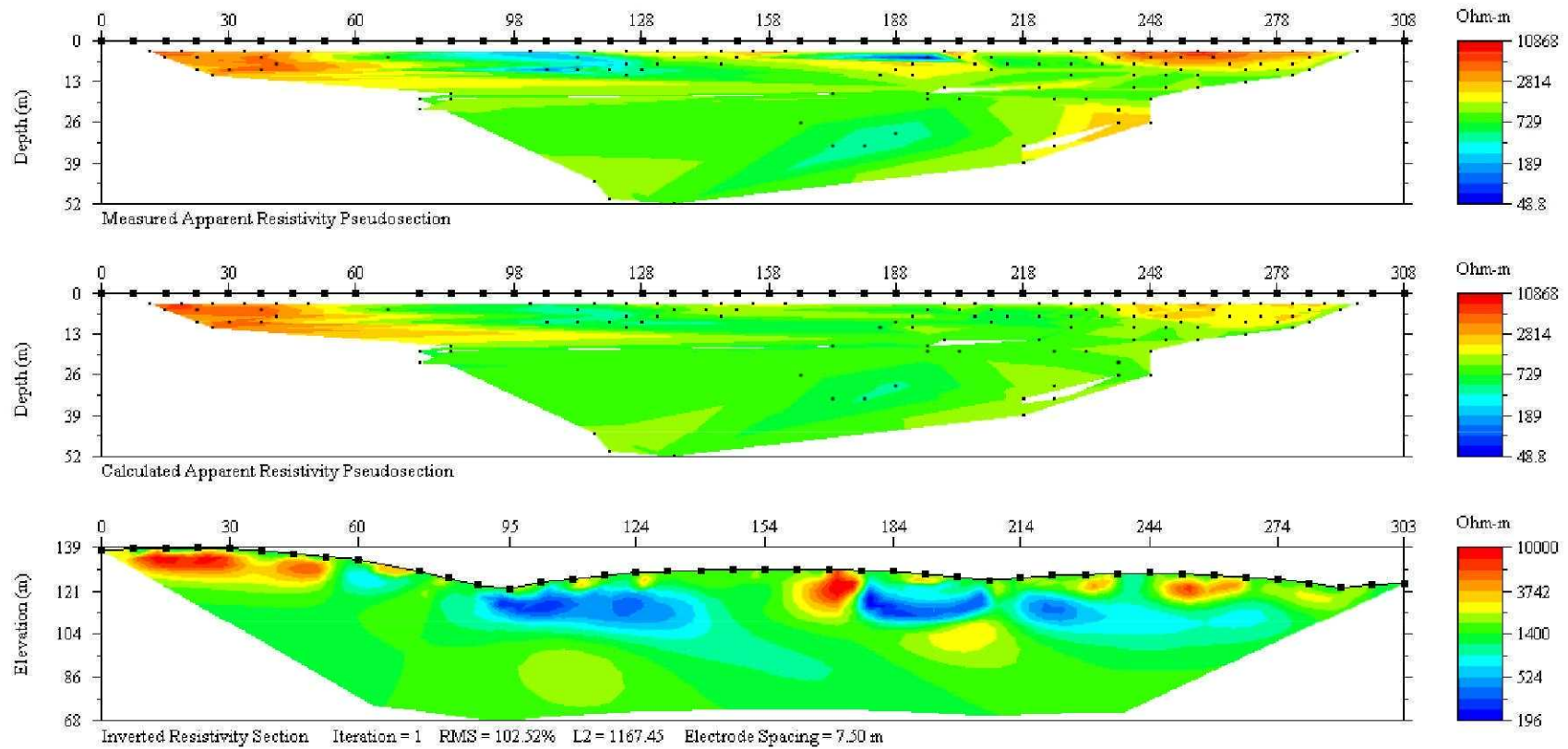
Profile 4 Resistivity Dipole-Dipole



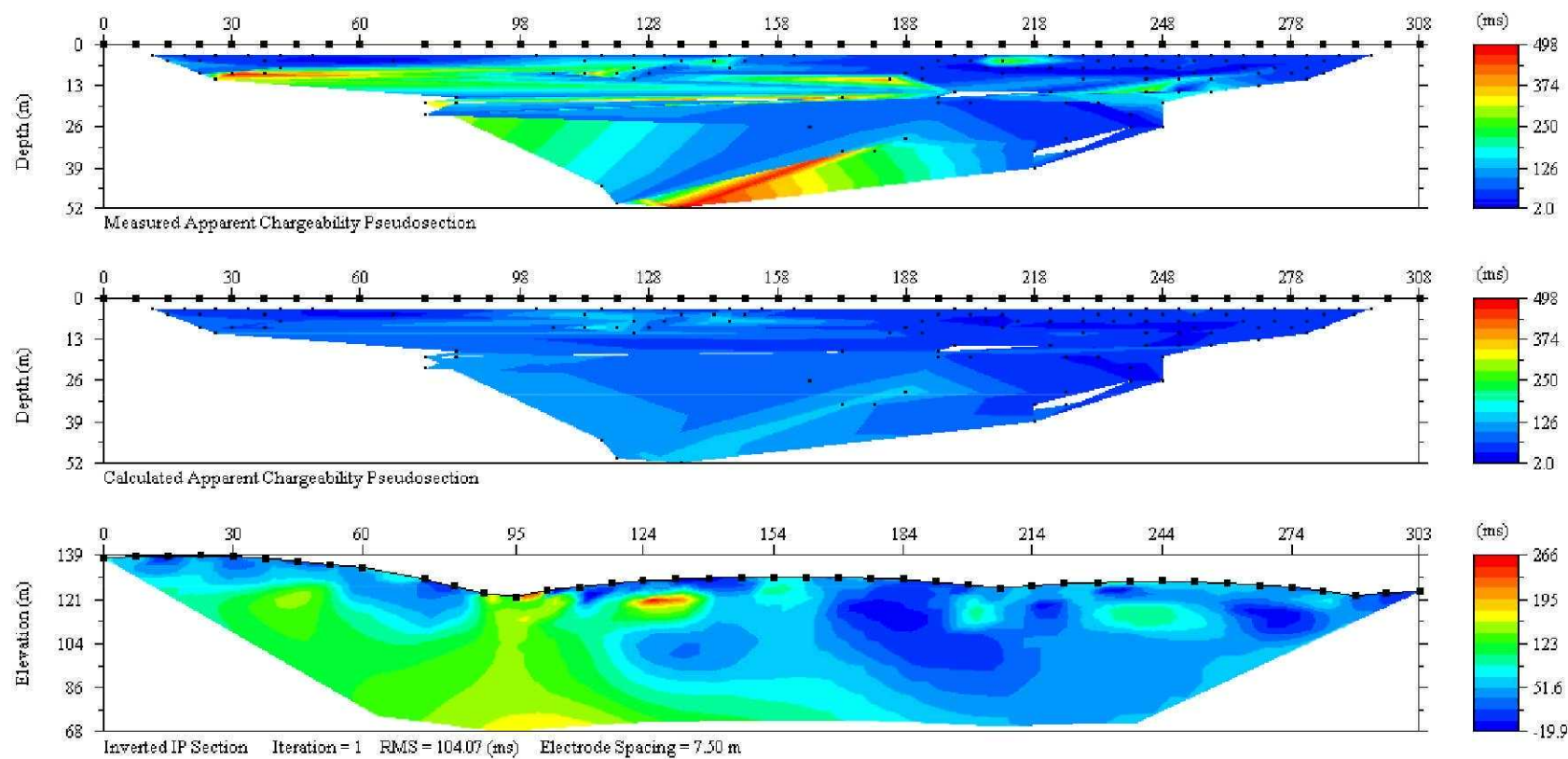
Profile 4 Induced Polarization Dipole-Dipole



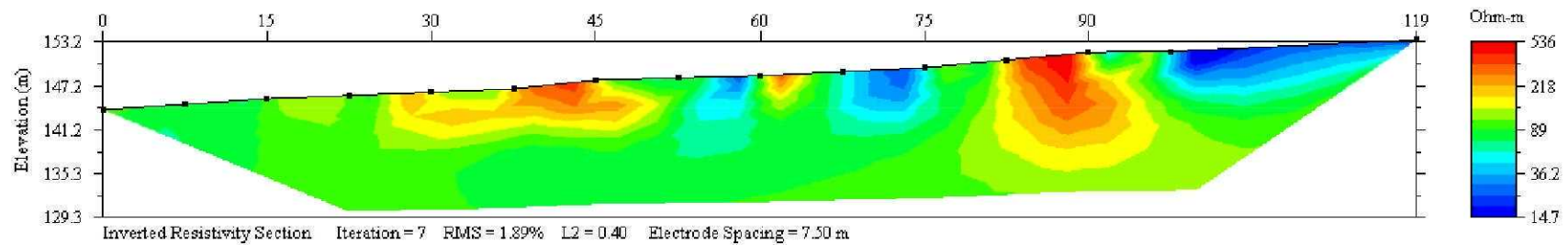
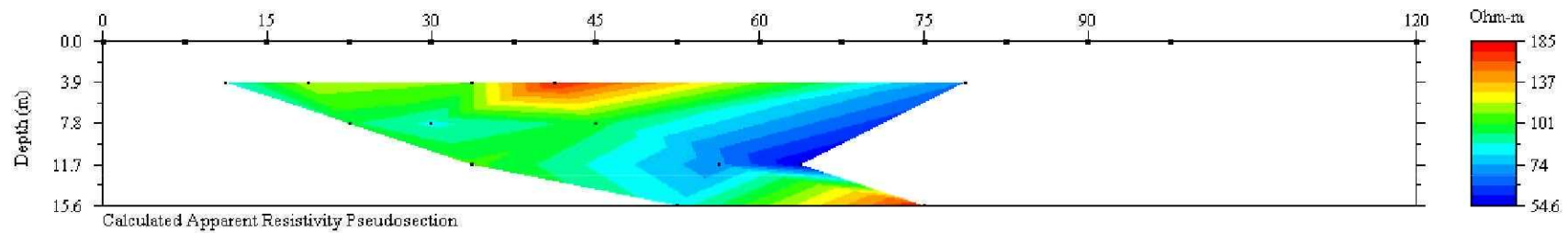
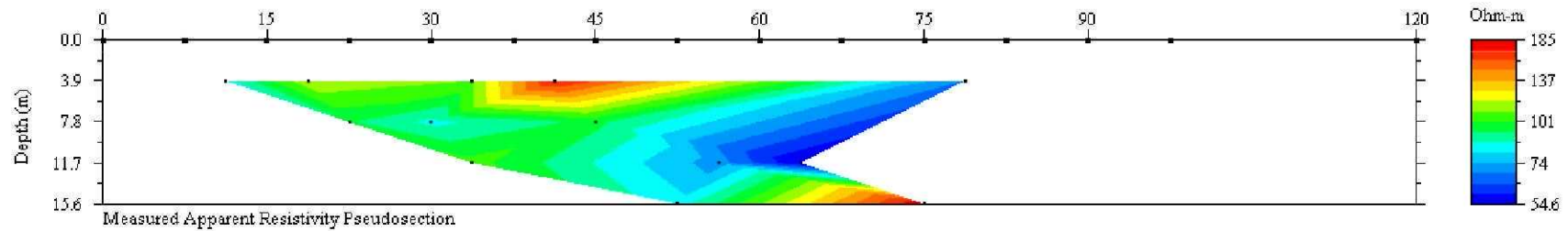
Profile 5 Resistivity Dipole-Dipole



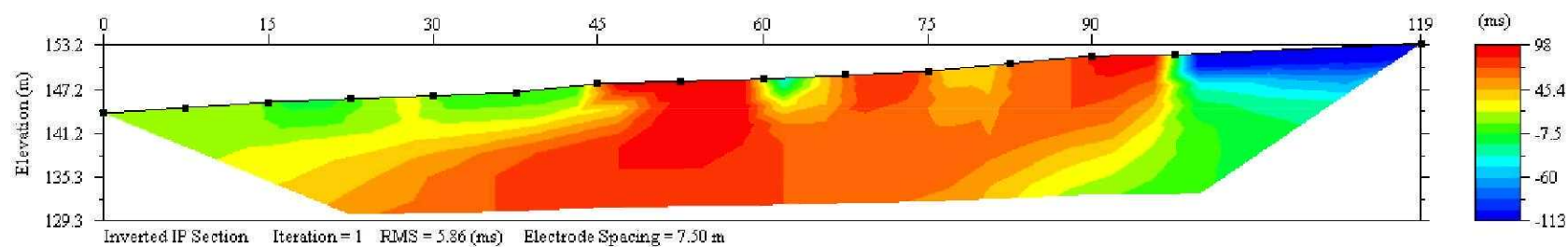
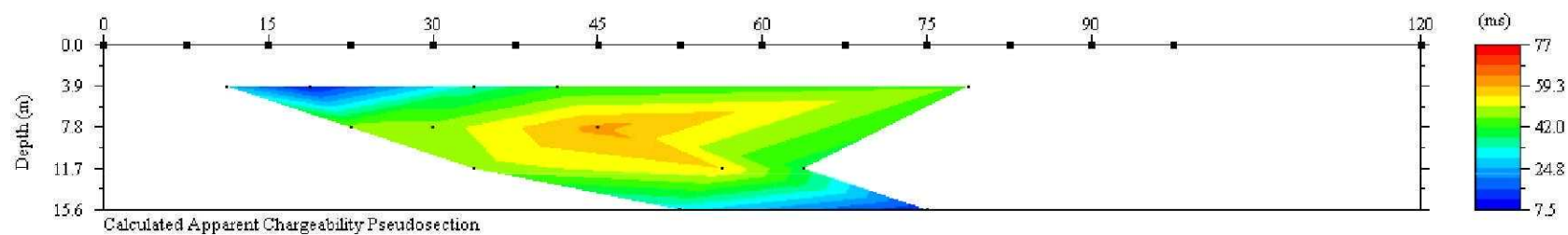
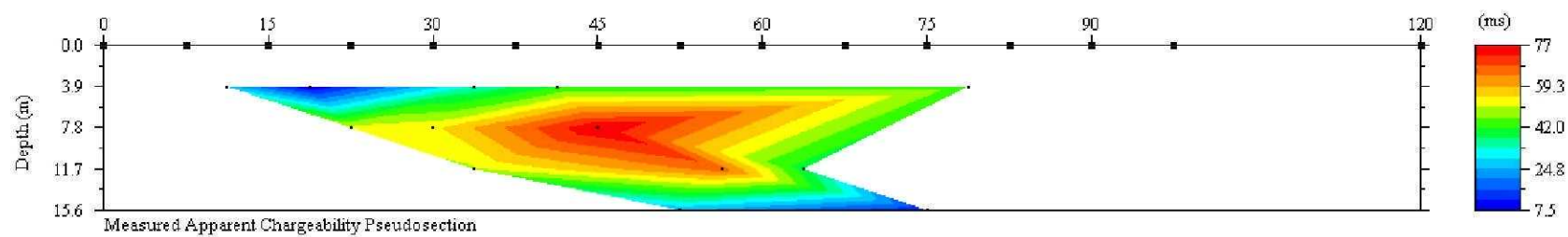
Profile 5 Induced Polarization Dipole-Dipole



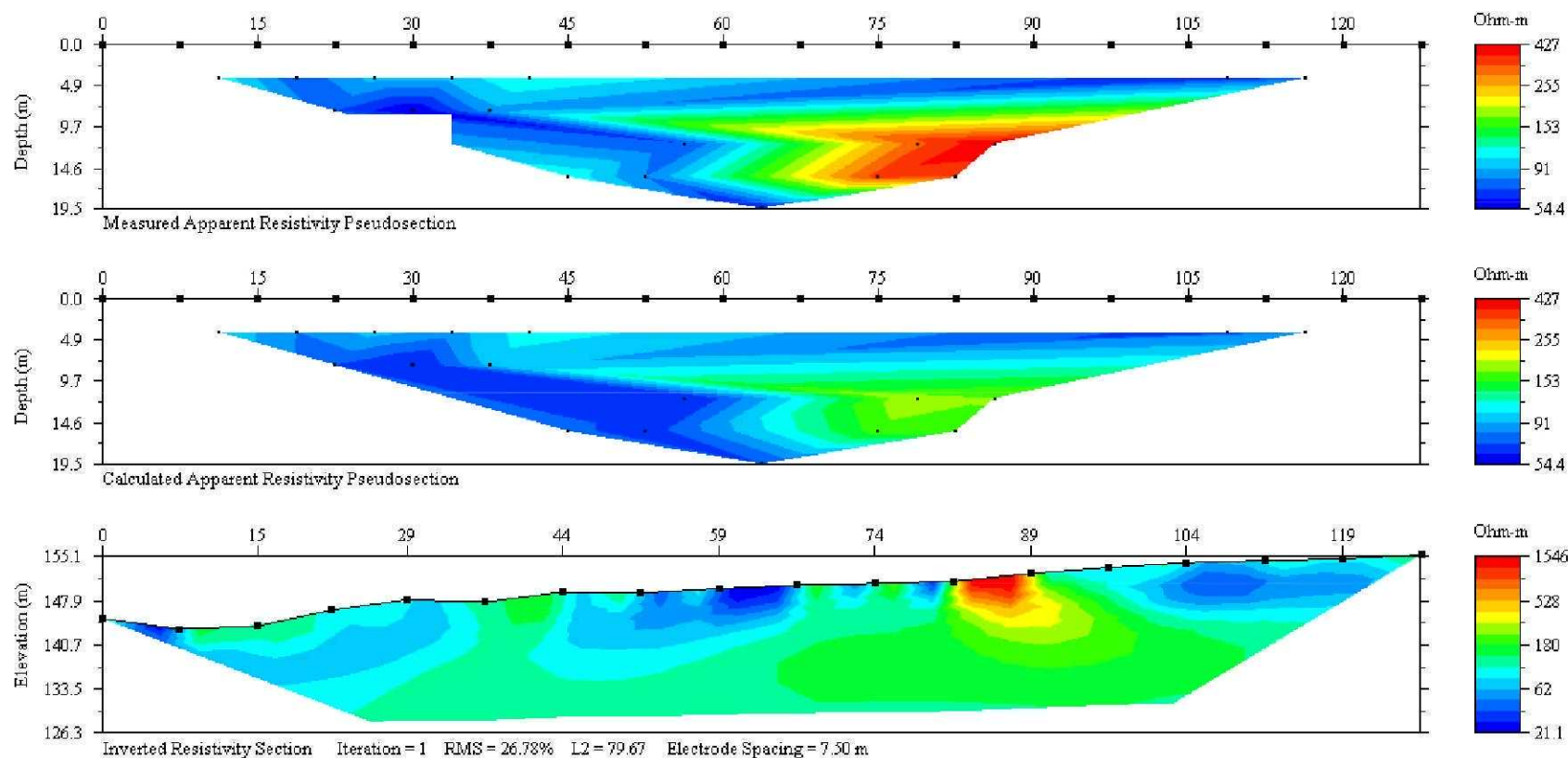
Profile 1 Resistivity Wenner



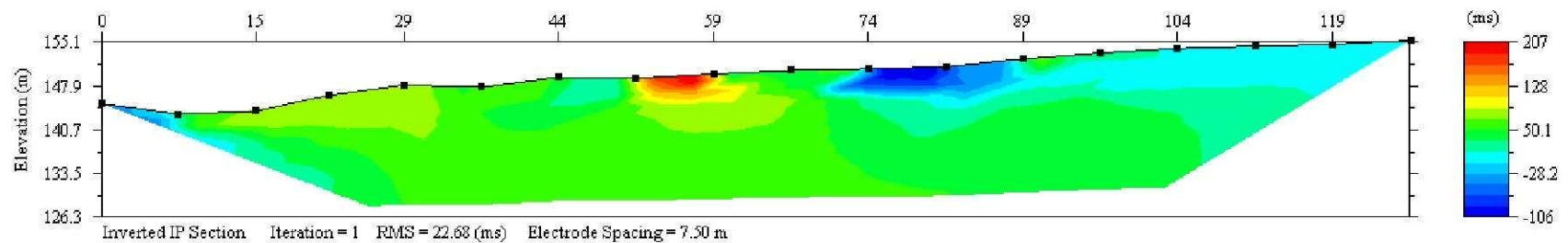
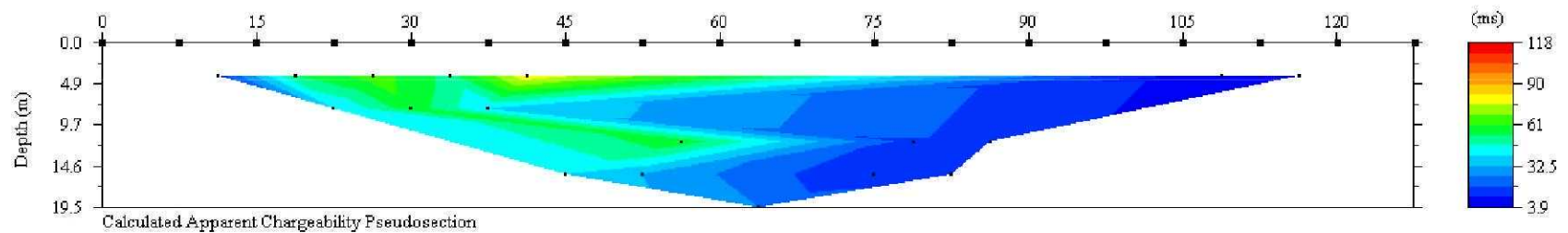
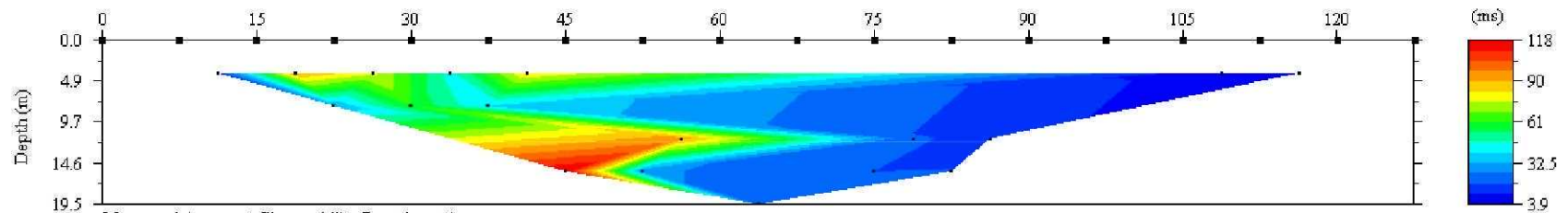
Profile 1 Induced Polarization Wenner



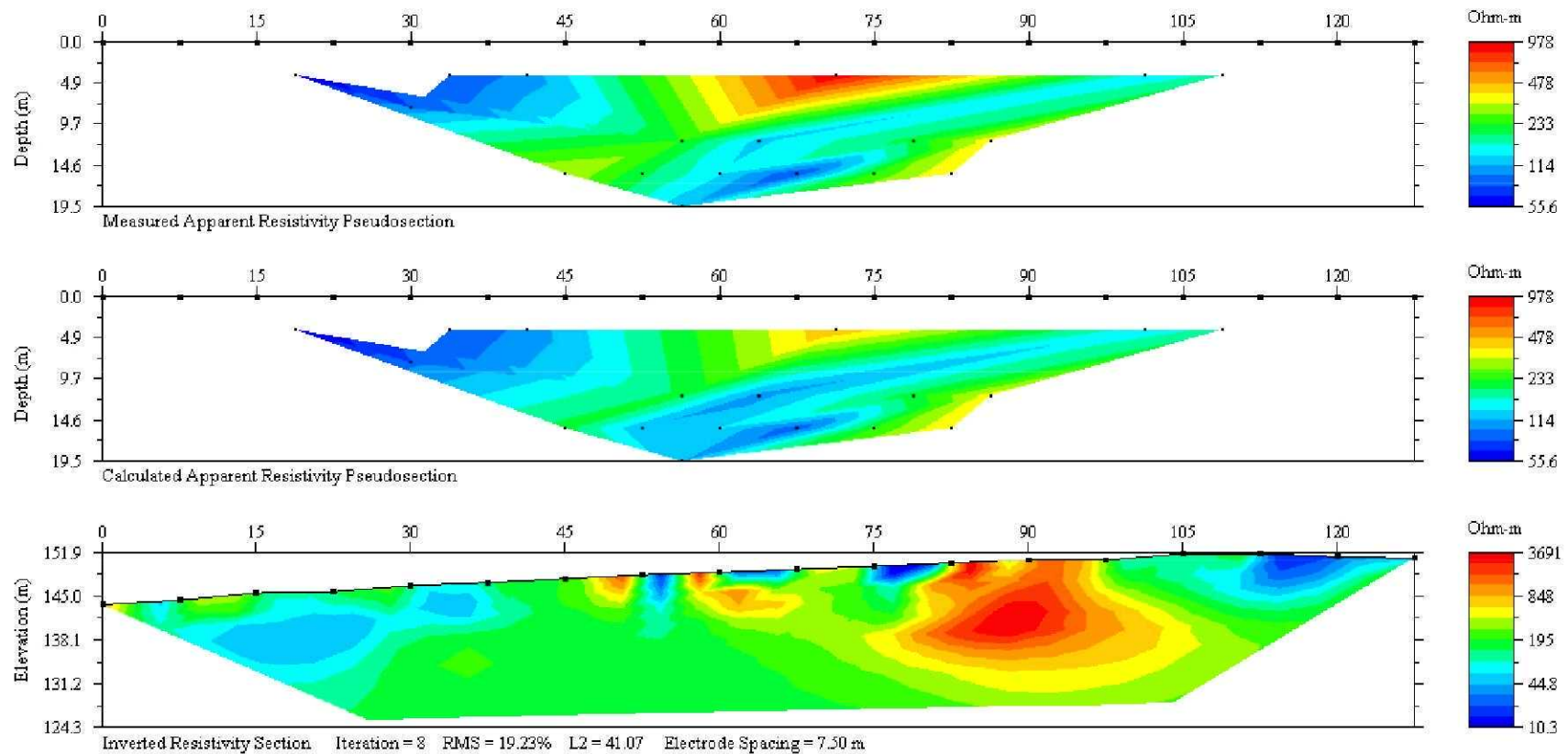
Profile 2 Resistivity Wenner



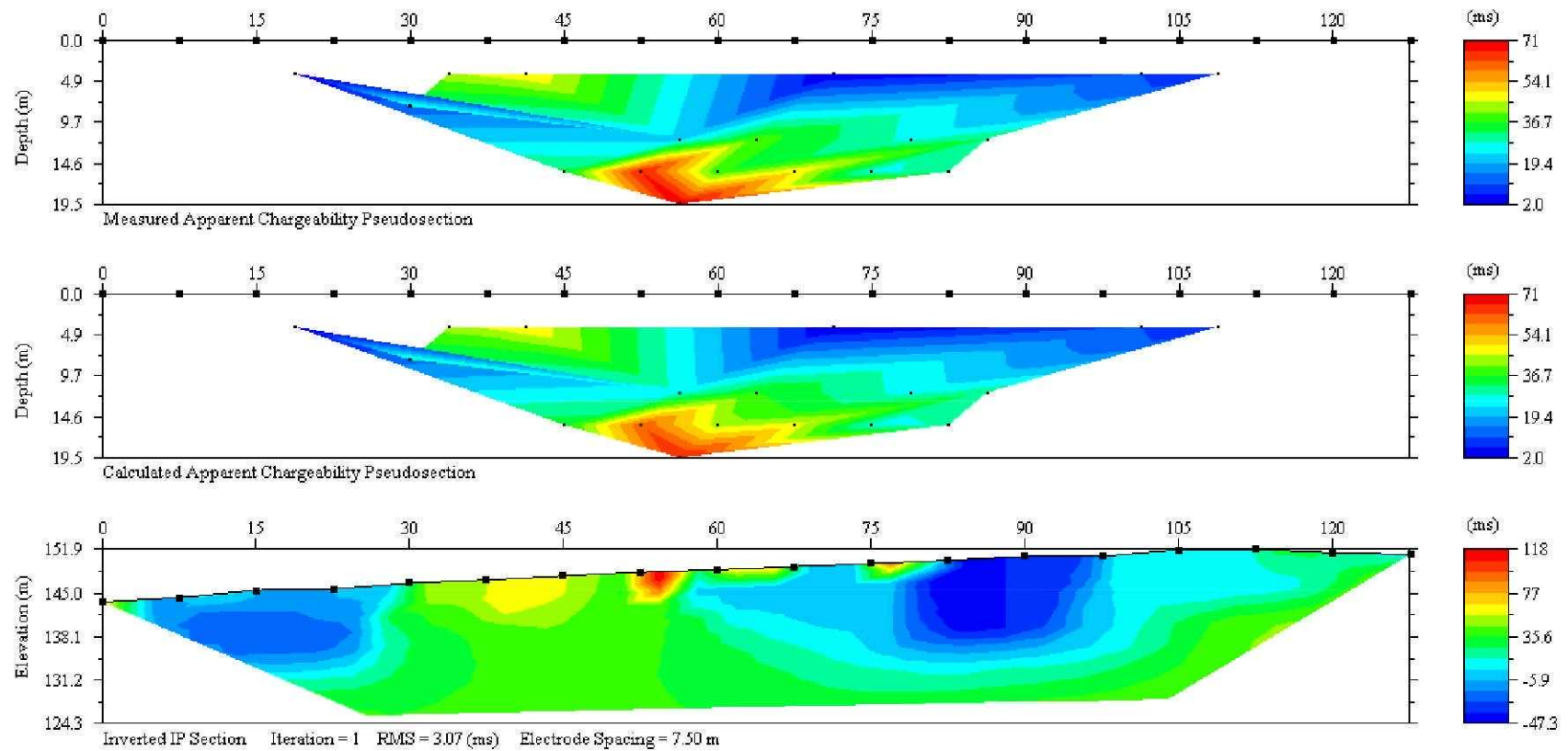
Profile 2 Induced Polarization Wenner



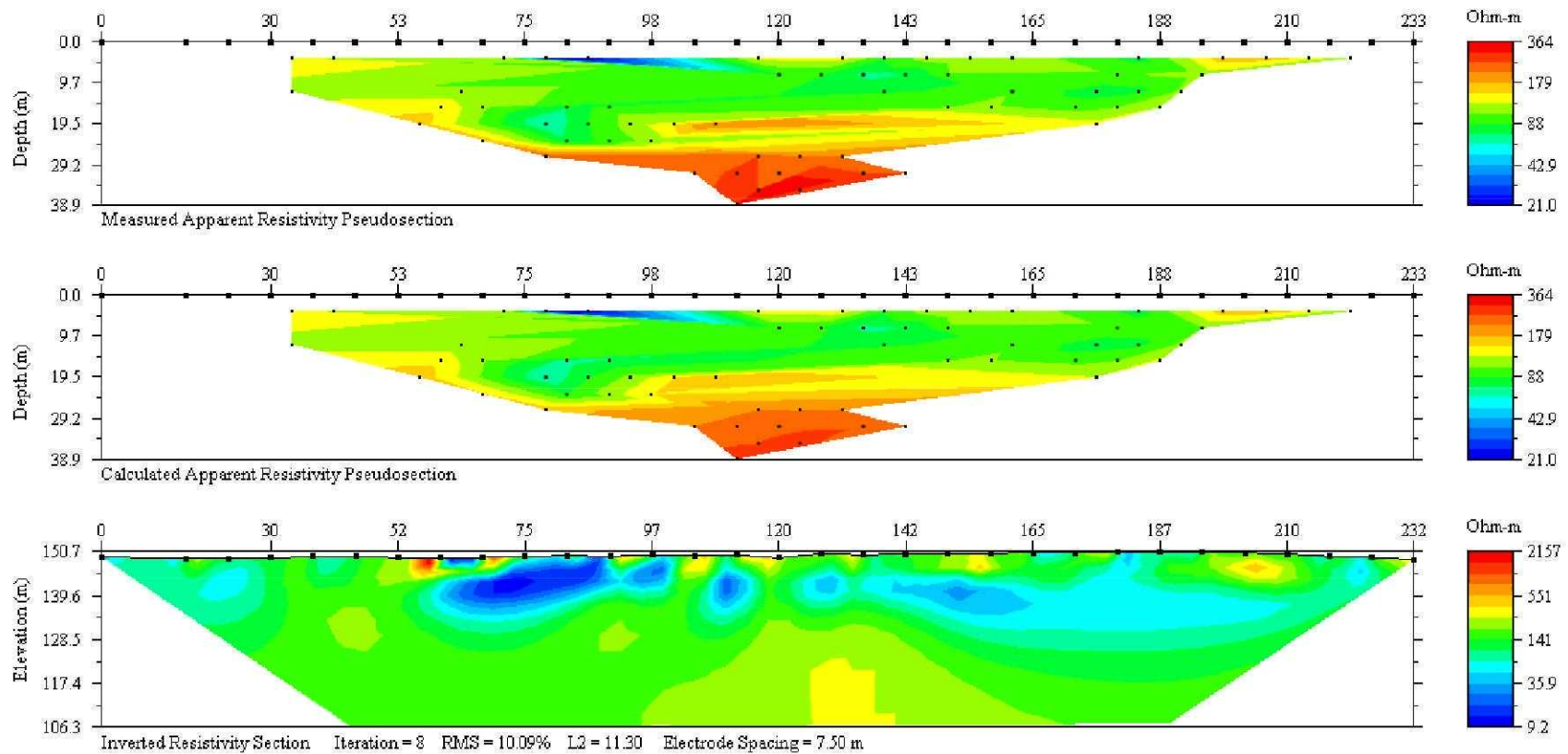
Profile 3 Resistivity Wenner



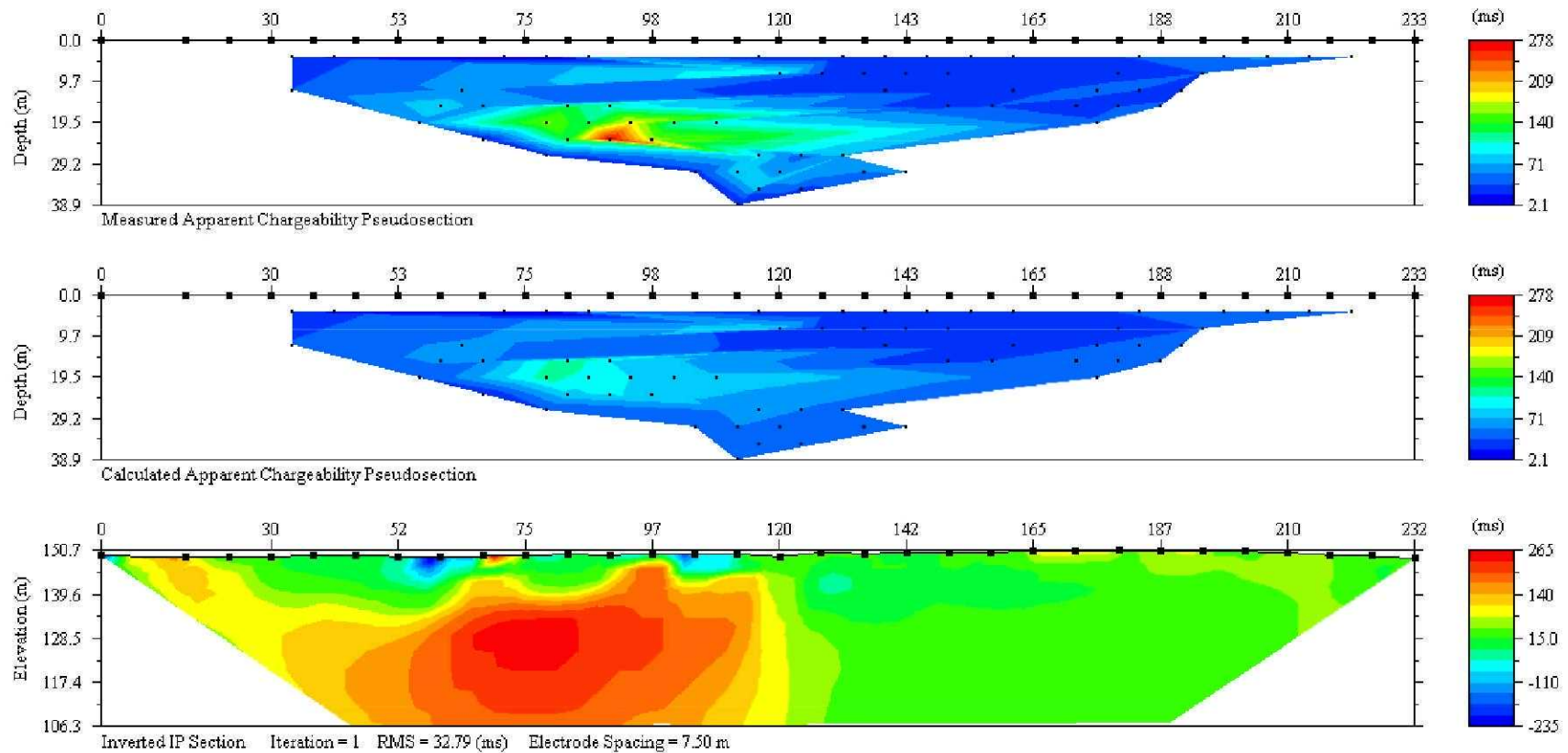
Profile 3 Induced Polarization Wenner



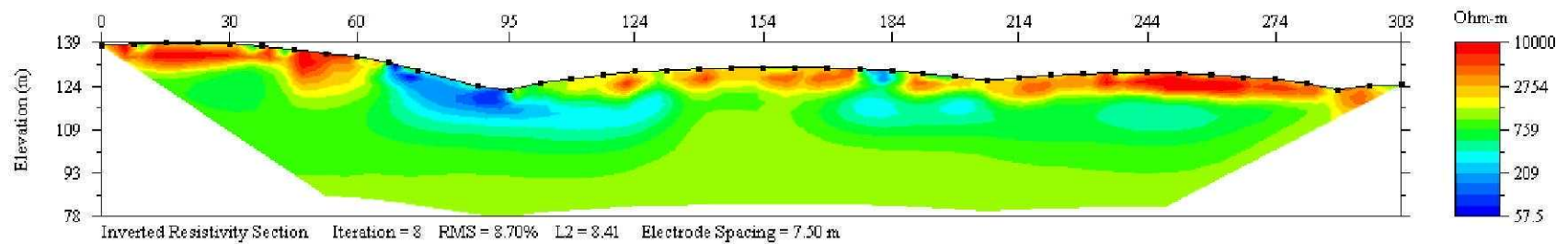
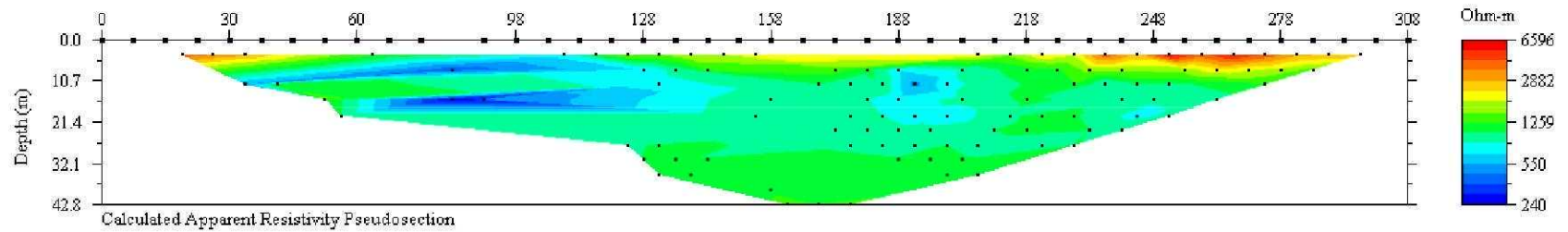
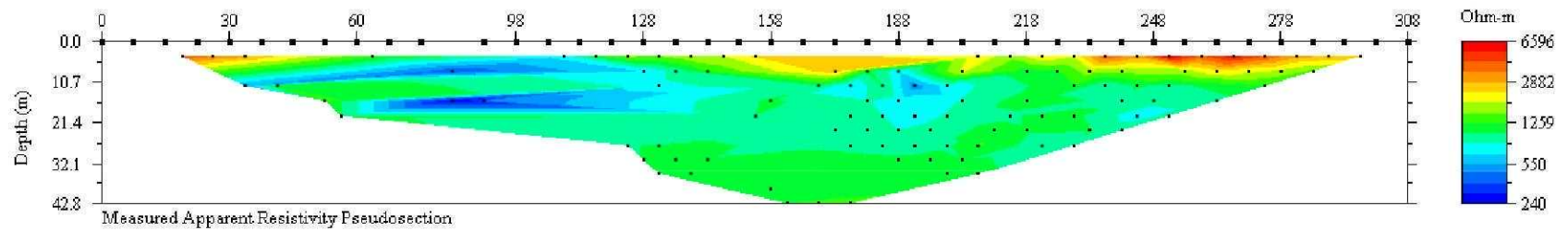
Profile 4 Resistivity Wenner



Profile 4 Induced Polarization Wenner



Profile 5 Resistivity Wenner



Profile 5 Induced Polarization Wenner

